NASA/TM—2015-218466 AIAA–2014–3675

# Three Orbital Burns to Molniya Orbit Via Shuttle/Centaur G Upper Stage

*Craig H. Williams*
*Glenn Research Center, Cleveland, Ohio*

March 2015

# NASA STI Program . . . in Profile

Since its founding, NASA has been dedicated to the advancement of aeronautics and space science. The NASA Scientific and Technical Information (STI) Program plays a key part in helping NASA maintain this important role.

The NASA STI Program operates under the auspices of the Agency Chief Information Officer. It collects, organizes, provides for archiving, and disseminates NASA's STI. The NASA STI Program provides access to the NASA Technical Report Server—Registered (NTRS Reg) and NASA Technical Report Server—Public (NTRS) thus providing one of the largest collections of aeronautical and space science STI in the world. Results are published in both non-NASA channels and by NASA in the NASA STI Report Series, which includes the following report types:

- TECHNICAL PUBLICATION. Reports of completed research or a major significant phase of research that present the results of NASA programs and include extensive data or theoretical analysis. Includes compilations of significant scientific and technical data and information deemed to be of continuing reference value. NASA counter-part of peer-reviewed formal professional papers, but has less stringent limitations on manuscript length and extent of graphic presentations.

- TECHNICAL MEMORANDUM. Scientific and technical findings that are preliminary or of specialized interest, e.g., "quick-release" reports, working papers, and bibliographies that contain minimal annotation. Does not contain extensive analysis.

- CONTRACTOR REPORT. Scientific and technical findings by NASA-sponsored contractors and grantees.

- CONFERENCE PUBLICATION. Collected papers from scientific and technical conferences, symposia, seminars, or other meetings sponsored or co-sponsored by NASA.

- SPECIAL PUBLICATION. Scientific, technical, or historical information from NASA programs, projects, and missions, often concerned with subjects having substantial public interest.

- TECHNICAL TRANSLATION. English-language translations of foreign scientific and technical material pertinent to NASA's mission.

For more information about the NASA STI program, see the following:

- Access the NASA STI program home page at http://www.sti.nasa.gov

- E-mail your question to help@sti.nasa.gov

- Fax your question to the NASA STI Information Desk at 757-864-6500

- Telephone the NASA STI Information Desk at 757-864-9658

- Write to:
  NASA STI Program
  Mail Stop 148
  NASA Langley Research Center
  Hampton, VA 23681-2199

NASA/TM—2015-218466 AIAA–2014–3675

# Three Orbital Burns to Molniya Orbit Via Shuttle/Centaur G Upper Stage

*Craig H. Williams*
*Glenn Research Center, Cleveland, Ohio*

Prepared for the
50th Joint Propulsion Conference
cosponsored by the AIAA, ASME, SAE, and ASEE
Cleveland, Ohio, July 28–30, 2014

National Aeronautics and
Space Administration

Glenn Research Center
Cleveland, Ohio 44135

March 2015

## Acknowledgments

The author would like to thank and acknowledge the considerable body of analytic research into the three burn problem by Dr. Keith Zondervon of The Aerospace Corporation, without which this analysis could not have been possible. Special thanks to Mr. Frank Spurlock (retired) of the NASA Lewis Research Center for his guidance and use of his renowned computer program DUKSUP, which was the generator of the data contained in this paper. Finally, special gratitude is extended to Colonel William Files, USAF, retired (Space Division) for the extraordinary opportunity to work on one of this nation's finest launch vehicle development programs: Shuttle/Centaur.

*Level of Review*: This material has been technically reviewed by technical management.

Available from

NASA STI Program
Mail Stop 148
NASA Langley Research Center
Hampton, VA 23681-2199

National Technical Information Service
5285 Port Royal Road
Springfield, VA 22161
703-605-6000

This report is available in electronic form at http://www.sti.nasa.gov/ and http://ntrs.nasa.gov/

# Three Orbital Burns to Molniya Orbit Via Shuttle/Centaur G Upper Stage

Craig H. Williams
National Aeronautics and Space Administration
Glenn Research Center
Cleveland, Ohio 44135

## Abstract

An unclassified analytical trajectory design, performance, and mission study was done for the 1982 to 1986 joint National Aeronautics and Space Administration (NASA)−United States Air Force (USAF) Shuttle/Centaur G upper stage development program to send performance-demanding payloads to high orbits such as Molniya using an unconventional orbit transfer. This optimized three orbital burn transfer to Molniya orbit was compared to the then-baselined two burn transfer. The results of the three dimensional trajectory optimization performed include powered phase steering data and coast phase orbital element data. Time derivatives of the orbital elements as functions of thrust components were evaluated and used to explain the optimization's solution. Vehicle performance as a function of parking orbit inclination was given. Performance and orbital element data was provided for launch windows as functions of launch time. Ground track data was given for all burns and coasts including variation within the launch window. It was found that a Centaur with fully loaded propellant tanks could be flown from a 37° inclination low Earth parking orbit and achieve Molniya orbit with comparable performance to the baselined transfer which started from a 57° inclined orbit: 9,545 versus 9,552 lb of separated spacecraft weight, respectively. There was a significant reduction in the need for propellant launch time reserve for a 1 hr window: only 78 lb for the three burn transfer versus 320 lb for the two burn transfer. Conversely, this also meant that longer launch windows over more orbital revolutions could be done for the same amount of propellant reserve. There was no practical difference in ground tracking station or airborne assets needed to secure telemetric data, even though the geometric locations of the burns varied considerably. There was a significant adverse increase in total mission elapsed time for the three versus two burn transfer (12 vs. 1¼ hr), but could be accommodated by modest modifications to Centaur systems. Future applications were discussed. The three burn transfer was found to be a viable, arguably preferable, alternative to the two burn transfer.

## Nomenclature

| | |
|---|---|
| $C_3$ | orbital energy per unit mass (from Newton's "vis viva" equation) |
| $L$ | mass ratio |
| $M$ | mass |
| $N$ | angle of perturbing thrust, in orbital plane, normal to motion |
| $R$ | radius |
| $T$ | angle of perturbing thrust, in orbital plane, tangent to motion |
| $V$ | velocity |
| $W$ | angle of perturbing thrust, normal orbital plane, positive where acceleration is positive |
| $a$ | semi-major axis |
| $e$ | eccentricity |
| $i$ | inclination |
| $l$ | semi latus rectum |

| | |
|---|---|
| $r$ | radius of instantaneous position |
| $t$ | time |
| $u$ | argument of the latitude ($\theta + \omega$) |
| $\Delta$ | change |
| $\theta$ | true anomaly |
| $\mu$ | product of Gravitational constant and mass of Earth = 62,748.55 $nmi^3/sec^2$ |
| $\Omega$ | node |
| $\omega$ | argument of the perigee |

**Subscripts**

| | |
|---|---|
| 2 | Burn 2 |
| 3 | Burn 3 |
| *a* | apogee |
| *D*1 | coast 1 drop mass |
| *D*2 | coast 2 drop mass |
| max | maximum |
| *p* | perigee |
| *PL* | payload |
| *prop* | propellant |
| *T* | total |

# 1.0 Introduction

An unclassified analytical trajectory design, performance, and mission analysis study was done for the 1982 to 1986 joint National Aeronautics and Space Administration (NASA)−United States Air Force (USAF) Shuttle/Centaur G upper stage development program to send performance-demanding payloads to high orbits such as Molniya. Motivated to mitigate a major concern at that time pertaining to the deployment of a significantly off-loaded Centaur stage from the Shuttle cargo bay, this orbital transfer method offered the potential to fill Centaur propellant tanks and secure comparable (or superior) performance compared to the baselined two burn transfer.

The Shuttle/Centaur upper stage development program of the 1980s was to produce the highest performing upper stages of that time. While the program produced two flight articles and was less than four months of launch, it (like many space systems) was a casualty of the repercussions of the Challenger Space/Shuttle accident of January 1986. Like many of the accomplishments of a fast moving space development and operational program, there was insufficient time to document noteworthy technical work. Following its cancellation, many of these achievements were left undocumented. During this fiftieth anniversary of the Centaur upper stage, this paper is an attempt to remedy one of these many achievements: the validation of a three orbital burns to Molniya orbit solution via Shuttle/Centaur G upper stage. Because of the unusual trajectory design and orbital mechanics involved, this subject could be of interest not just for historical reasons, but possible application to future launch vehicles as well.

# 2.0 Background

## 2.1 Shuttle/Centaur G Upper Stage and Its Missions

Shuttle/Centaur was a joint NASA and USAF upper stage development program initiated in July 1982 (with some early work in 1981). Based on the existing, highly successful Atlas/Centaur upper stage, Shuttle/Centaur was to be an expendable system (with its origin in unmanned space system) used by the partially reusable Space Shuttle system (a manned space system) (Ref. 1). This was to be another

successful teaming of experienced expendable launch vehicle development organizations: NASA Lewis Research Center (LeRC, now NASA Glenn Research Center (GRC)), USAF/Aerospace Corporation, and General Dynamics Corporation. This government and industry team developed two versions of Shuttle/Centaur upper stages: the smaller "G" version primarily for national security missions and the larger "G-Prime" version designed primarily for NASA interplanetary missions. Compared to other launch vehicles at the time, Shuttle/Centaur represented a doubling of performance capability for comparable missions. A joint program office was established at Cleveland's NASA LeRC with a co-located USAF Space Division detachment. The same Atlas/Centaur major contractors were retained: General Dynamics (Centaur stage), Pratt & Whitney (RL10 engines), Teledyne (Digital Computer Unit and other avionics), and Honeywell (Inertial Navigation Unit and other avionics) (Ref. 2).

Shuttle/Centaur G and its payload were to be cradled by the Centaur Integrated Support System (CISS) within the Shuttle cargo bay. The CISS and the forward attach points supported the upper stage and payload from Space Shuttle mating through cargo bay deployment on-orbit. Once in orbit, with cargo bay doors opened, the CISS rotated the Centaur/payload to the deployment angle and the Centaur/payload were deployed. Figure 1 is an artist's conception of a Shuttle/Centaur G and payload in low Earth orbit following deployment from the Space Shuttle's cargo bay. Shuttle/Centaur would then maneuver to a predetermined safe location, fire its engines, and inject the spacecraft to the desired orbit. The first two missions (each using the G-Prime version) were the Galileo mission to Jupiter and the International Solar Polar Mission (renamed Ulysses) to the Sun. Both missions were slated for launch within days of each other in May 1986.

The Shuttle/Centaur program made rapid progress. Within 3½ years following authority to proceed, two G-Prime flight vehicles had been designed, developed, manufactured, tested, integrated, and were being prepared for launch at the Cape. A pathfinder test article had also been built and preceded them. In addition, two G flight vehicles were approximately 50 percent complete by that same time. Figure 2 illustrates the G-Prime rollout at the General Dynamics plant in Kearny Mesa, California in 1985.

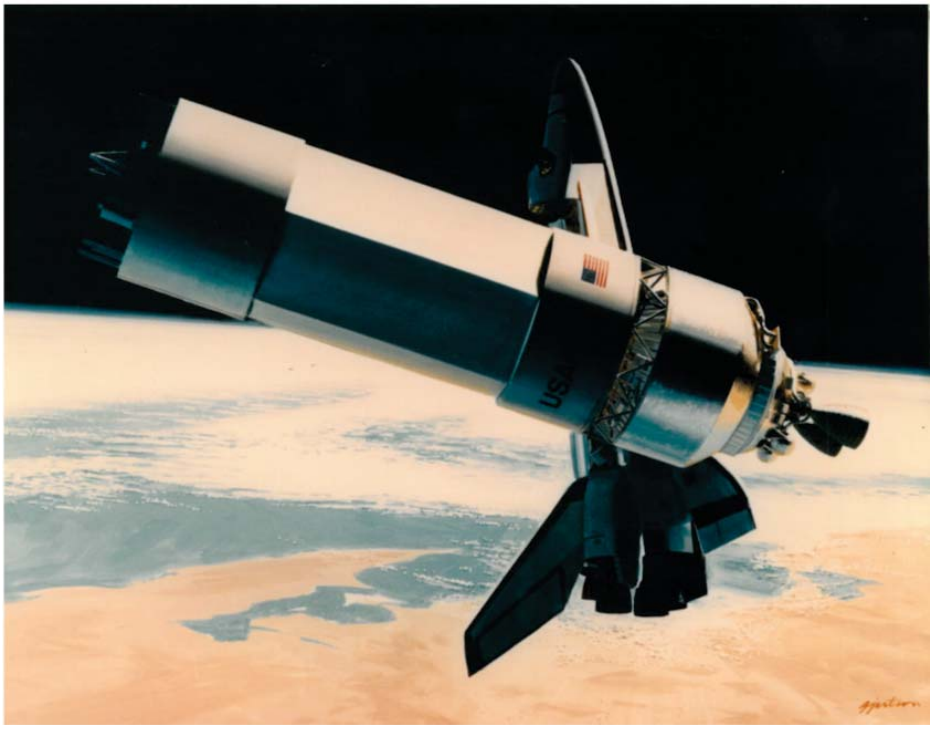

Figure 1.—Artist's View of Deployed Shuttle/Centaur G with Payload.

Figure 2.—Shuttle/Centaur G-Prime Rollout at General Dynamics in 1985.

Despite the cancellation of the Shuttle/Centaur program following the Space Shuttle Challenger disaster in 1986, the Shuttle/Centaur G-Prime vehicle was quickly adopted by the USAF/Space Division and integrated with its new Titan IV booster. From 1994 to 2003, the Titan IV/Centaur was launched 16 times: 14 were successful, one experienced a Centaur failure, and one experienced a Titan IV core failure (i.e., Centaur no-trial). One of the Titan IV/Centaur missions was the 1997 launch of the Cassini spacecraft to Saturn. This was NASA LeRC's last launch, ending its 35 year tenure leading NASA's expendable launch vehicle program. Shuttle/Centaur G-Prime (integrated with the Titan IV) remains to this day the last launch vehicle NASA has developed, integrated, and launched successfully.

Data from unclassified publications (Refs. 3, 4, 5, 6, and 7) of the time describe the vehicle system and performance used to model the Shuttle/Centaur G vehicle system and the two 'generic' missions to which its performance was measured against. One of these was the 12 hr Molniya orbit—an orbit which provided long (~ 10 hr) dwell times over a land mass. Shuttle/Centaur G's performance requirement to a generic Molniya orbit was 11,500 lb. Another major requirement was to accommodate a 40-ft long payload within the existing 60-ft long Shuttle cargo bay. This requirement was the primary reason for the 10-ft shorter G version (compared to the longer G-Prime). The drawing in Figure 3 compares the G and G-Prime vehicles. The G's shorter, smaller tanks could only accommodate a nominal 30,000 lb propellant load (compared to the G-Prime's nominal 45,000 lb). This meant that a new version of the RL10 engine was needed to burn the propellants at a 6:1 mixture ratio rather than the heretofore standard of 5:1.

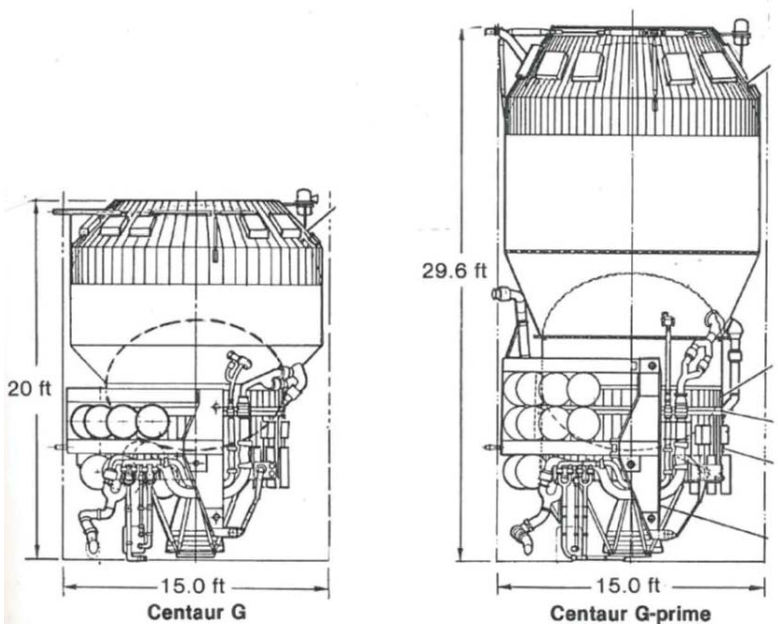

Figure 3.—Comparison of Shuttle/Centaur G and G Prime.

## 2.2 Problem Statement

Like all launch vehicles, the Space Shuttle lift capability was degraded as its launch azimuth (LAZ) was decreased from 90° due East. This was because as LAZ was lowered to increase the parking orbit inclination (assuming planar ascent), the smaller became the useful component of Earth's rotational velocity to achieve orbit, thus the lower the payload capability. In order to maximize payload to Molniya orbit, the lowest LAZ available from NASA's Kennedy Space Center (35°) was used for planar ascent to reach the maximum parking orbit inclination (57°). While this minimized the amount of plane change performed by the upper stage to reach the final 63.4° inclination Molniya orbit, it also severely reduced the Shuttle lift commitment by 16,600 lb. This decrease in Shuttle capability forced a severe (~ 40 percent by weight) offload of Centaur's total tankable propellants, resulting in a tremendous performance hit for the launch system.

This considerable off-load of Centaur propellants raised three major concerns for the mission planners:

- The possibility of large scale dynamic instabilities associated with deploying a considerably offloaded Centaur due to unsettled propellants "sloshing' in the tanks could have led to an unstable deployment, and possibly a dangerous recontact with the Space Shuttle. There was a strong desire to find a way to reduce the propellant off-load (i.e., fill the tanks) to ameliorate the problem, and also preclude the need to add slosh baffles which would increase dry weight. But an alternate approach implied a greater LAZ (to enable a greater Shuttle cargo element weight limit). An alternate transfer could preclude a complicated analysis designed to determine where the propellants would be located in the tank prior to deployment. In addition, any analysis on a significantly offloaded tank might have been more severely affected by tanking dispersions or late deployment than a fully loaded mission. Thus a study was initiated to discover an alternate approach to mitigate this problem. This concern was the primary motivation for exploring alternate transfers to Molniya orbit.
- Shuttle/Centaur's performance was significantly degraded due to the propellant offload. There was a strong interest to find an alternate trajectory to enable a greater payload to Molniya orbit.

- Launch windows were expected to be costly in terms of propellant margins which would have to be held in reserve. This was due to the high inclination parking orbit and its performance cost for out of plane yaw steering needed to generate the windows. Contributing to this problem, deployment from the cargo bay could be delayed until the seventh revolution (or even later ('second day deployment')) due to the nature of Shuttle/Centaur space operations. If a way could be found to lessen the amount of out of plane (yaw) steering and accommodate multiple revolutions, a greater payload to final orbit should have been possible.

To address these three major concerns, four analyses were performed for the generic Molniya mission:

- Physics of an alternate transfer and comparison to the standard transfer
  Performance of both transfers for a range of park orbit inclinations
- Performance for launch windows up to 1½ hr and deployment revolutions 5, 6, and 7
- Ground tracks for nominal transfers and range of main burns throughout the launch windows

## 2.3 Origins of the Three Orbital Burns to Molniya Orbit Solution

The generic Molniya orbit has an:

- 14,340 nmi semi-major axis (which dictates a 12-hr period)
- 500 nmi perigee radius altitude (alt) (which defines the highly eccentric orbit, providing long dwell times (~10 hr) over a specified land area (centered about apogee)
- 63.4° inclination (which eliminates the precession of the line of apsides)
- 270° argument of the perigee (which positions the long dwell time over the greatest northern latitudes)

The baseline 2B transfer to Molniya orbit via Shuttle/Centaur G is illustrated in Figure 4.

In the field of orbital mechanics and trajectory design, it is known that a class of optimal orbital transfers exist utilizing three burns ("3B") following insertion into a low Earth parking orbit (LEO) for missions such as Molniya. While two orbital burn ("2B") solutions are more conventional, 3B transfers have more degrees of freedom from which to yaw out of plane to satisfy requirements of angular orbital elements and enabling the possibility for greater performance. If a transfer could be found which started from a lower parking orbit inclination, a greater Shuttle lift capability could permit the filling of Centaur tanks. This would require Centaur to do more of the plane change, but a more efficient 3B transfer might enable a greater overall system performance.

The Ph.D thesis by Dr. Keith P. Zondervan of The Aerospace Corporation was used as the starting point for the baseline 3B trajectory for this analysis. Titled "Optimal Low Thrust, Three Burn Orbit Transfers with Large Plane Changes," Dr. Zondervan's thesis contained comprehensive material and detailed formulations of the optimal control and two point boundary value problems of orbital transfers (Ref. 8). The necessary conditions for the generalized problem were defined for both a "thrust-limited" case and an "acceleration-limited" case. Three methods of solving the two optimal control problems were given. The thesis worked through three lengthy example problems, each with a different initial and final orbit pair, and each with "thrust-limited" and "acceleration-limited" solutions. The examples also provided parametric data for various initial thrust-to-weight and final perigees. One of the comprehensive example problems was a 3B transfer from LEO to Molniya orbit.

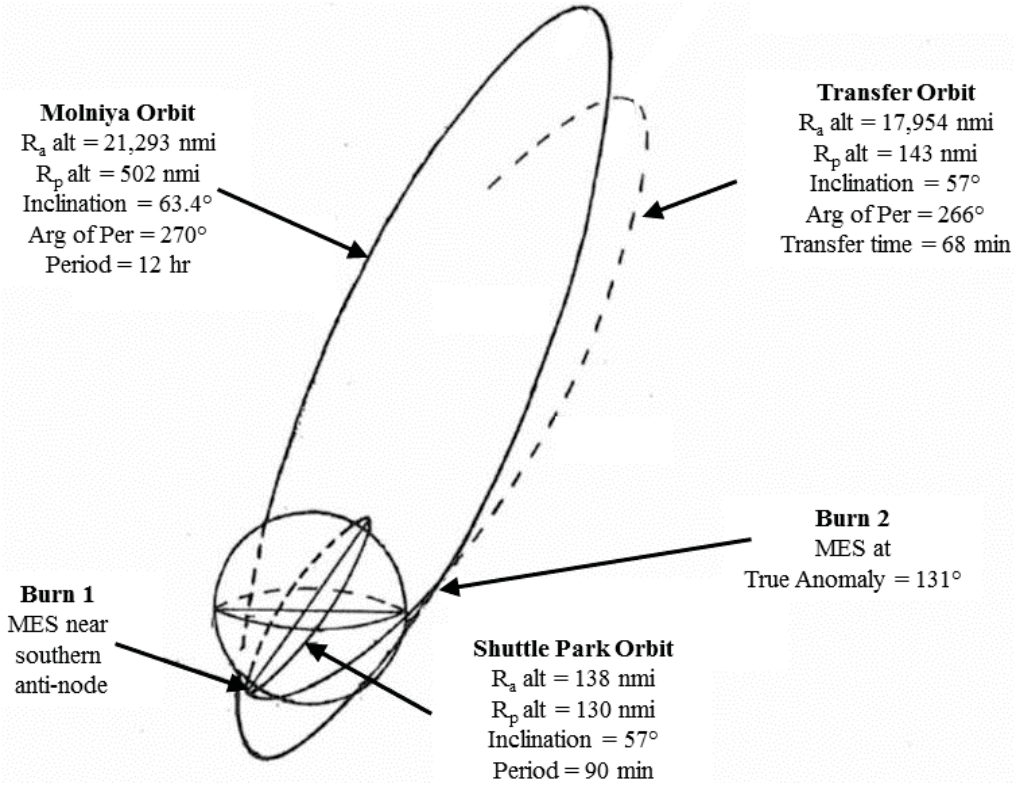

Figure 4.—Two Burn Transfer to Molniya Orbit.

The baseline 3B trajectory and transfer orbit characteristics for the Molniya transfer were obtained from the Zondervan thesis ("Aerospace solution"), and used as the target solution to converge to by the NASA analytical model. The specific Aerospace solution used was the example problem: inclination = 28.5° circular to 63.4° elliptic transfer (acceleration-limited solution) given in Tables 18 and 23 of the thesis. These data are for thrust to weight ($T/W$) of 1.0, which was equivalent to that of the Shuttle/Centaur G for the generic Molniya mission, except for $R_p$ alt = 300 nmi. (Note: typographical errors exist in initial orbit inclination in Table 23 of Ref. 8.) Since no actual propulsion system was modeled in the thesis, the initial $T/W$ and "acceleration-limited" relation served as proxies for the operational definition of the propulsive stage. The initial NASA analytic model (vehicle and trajectory) of the Shuttle/Centaur G was the existing high fidelity model for the generic 2B solution for a Molniya transfer. The model was created within NASA LeRC's 3D computer program DUKSUP: a calculus of variations-based algorithm used to design high fidelity, optimized launch trajectories for Atlas/Centaur and Titan/Centaur vehicles for over 15 years (Refs. 9 and 10). In order to first match the Aerospace solution, the "NASA GRC" model was simplified to eliminate detailed vehicle operation characteristics (such as hardware drops, propellant boiloffs/ventings/settlings, pre-chill/pre-start, and startup/shutdown transients). Then, the second burn was adjusted simultaneously as the third burn was introduced into the GRC model. Gradually, the GRC model was iterated to converge to the Aerospace solution of the three burn transfer.

Table 1 (columns 1and 2) contains the elements of the parking, transfer, and final orbits for both Aerospace and GRC 3B baseline transfers, as well as the other data to be discussed in a later section. Consistent with other contemporary analytically modeled missions, a slightly elliptical parking orbit (160- by 148-nmi alt) was maintained in the GRC model, where the Aerospace solution used a circular orbit

(150- by 150-nmi alt). Also, the Aerospace model used a simplified park orbit model, where the other orbital elements were set to zero (Table 1).

There was good agreement with each orbital element in each of the orbits for the Aerospace and GRC models (with the exception of node, which was reference frame and initial state vector dependent) (Table 1). With the agreement between the two 3B transfer models established, the analysis was then ready for re-introduction of the detailed Centaur propulsive characteristics (i.e., hardware drops, propellant boiloffs, settlings, etc.) as well as the adjustments to parking and final orbit state conditions, and the other analysis ground rules.

## 2.4 Analysis Ground Rules

Two sets of slightly different initial and final orbits were used in this study. In the comparison of the Aerospace Corporation's 3B transfer to that of GRC's 3B transfer (see preceding section), a Space Shuttle 150 nmi near circular, 28.45° inclined parking orbit to a 300 nmi perigee altitude Molniya orbit transfer was used (Refs. 3 and 4). These data are the first and second columns in Table 1. For the comparison of the GRC 3B transfer to the standard 2B transfer, inclination variation analyses, launch window analyses, and ground track assessments, a slightly different set of initial and final orbits were used (Ref. 5, 6, and 7). The data of these transfers are the third and fourth columns in Table 1. The 3B data was taken from Reference 3 ("mini-Colt") and 2B data was taken from Reference 7 ("Colt"). (Note: almost all of the data contained in this paper is archival, originally created by the author, but with no practical way to easily rerun any of the analyses due to obsolete software. Thus, some gaps in the analysis appear in this paper.) Figure 5 illustrates the baseline 3B transfer to Molniya orbit represented by column 3 (mini-Colt data) in Table 1.

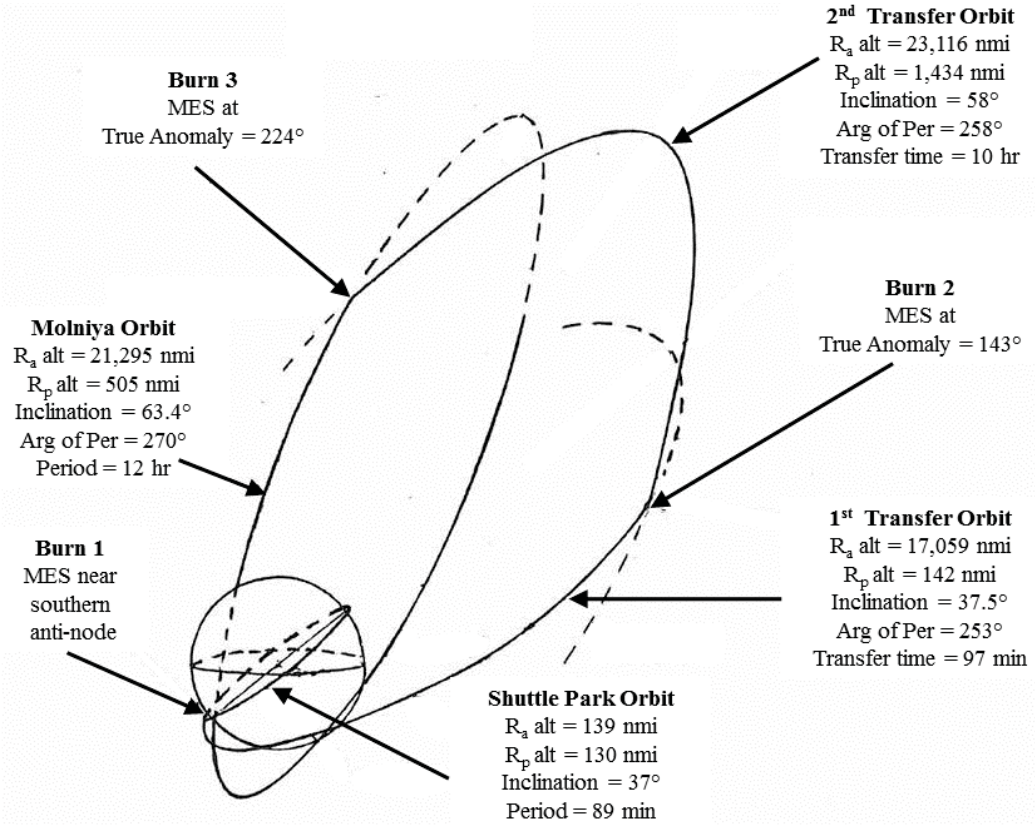


Figure 5.—Three Burn Transfer to Molniya Orbit.

TABLE 1.—ORBITAL ELEMENTS OF THREE AND TWO BURN TRANSFERS

| | 3 Burn Aerospace Ph.D Thesis | 3 Burn NASA GRC | 3 Burn Aug. 1984 mini-Colt | 2 Burn Oct. 1985 Colt |
|---|---|---|---|---|
| Parking orbit of period (hr) | 1.5 | 1.5 | 1.5 | 1.5 |
| Apogee altitude (nmi) | 150.0 | 160.3 | 139.1 | 138.3 |
| Perigee altitude (nmi) | 150.0 | 147.7 | 130.4 | 130.4 |
| Inclination (deg) | 28.5° | 28.5° | 37.0° | 57.0° |
| Argument of Perigee (deg) | 0.0° | 206.8° | 3.4° | –0.7° |
| True Anomoly (deg) | 0.0° | 36.1° | –2.8° | 0.7° |
| Node (deg) | 0.0° | 189.4° | 189.7° | 2.0° |
| Start 1st transfer orbit; coast duration (hr) | 2.3 | 2.3 | 1.6 | 1.1 |
| Apogee altitude (nmi) | 20,355.7 | 20,403.8 | 17,059.4 | 17,953.8 |
| Perigee altitude (nmi) | 153.4 | 146.8 | 142.0 | 142.6 |
| Inclination (deg) | 29.1° | 29.1° | 37.5° | 57.0° |
| Argument of Perigee (deg) | 247.7° | 247.7° | 252.7° | 266.2° |
| True Anomoly (deg) | 6.9° | 7.0° | 10.5° | 8.2° |
| Node (deg) | 3.2° | 192.6° | 191.3° | 2.0° |
| Start 2nd transfer orbit; coast duration (hr) | 12.2 | 12.2 | 10.1 | --- |
| Apogee altitude (nmi) | 26,550.9 | 26,556.5 | 23,115.8 | --- |
| Perigee altitude (nmi) | 2,135.8 | 2,132.6 | 1,433.8 | --- |
| Inclination (deg) | 57.4° | 57.4° | 58.3° | --- |
| Argument of Perigee (deg) | 248.4° | 248.4° | 258.2° | --- |
| True Anomoly (deg) | 133.0° | 133.0° | 127.4° | --- |
| Node (deg) | 26.5° | 215.9° | 207.9° | --- |
| Molniya final orbit of period (hr) | 12.0 | 12.0 | 12.0 | 12.0 |
| Apogee altitude (nmi) | 21,500.0 | 21,492.5 | 21,295.2 | 21,292.8 |
| Perigee altitude (nmi) | 300.0 | 299.9 | 504.9 | 502.1 |
| Inclination (deg) | 63.4° | 63.4° | 63.4° | 63.4° |
| Argument of Perigee (deg) | 270.0° | 270.0 | 270.0 | 270.0 |
| True Anomoly (deg) | 215.3° | 215.3 | 217.0 | 124.9 |
| Node (deg) | 15.7° | 205.2° | 199.6° | 7.3° |
| Burn characteristics | | | | |
| Burn 1 time (sec) | 193.4 | 190.9 | | |
| Coast arc 1-2 (deg) | 144.1° | 144.0° | | |
| Burn 2 time (sec) | 69.5 | 67.9 | | |
| Coast arc 2-3 (deg) | 98.5° | 98.5° | | |
| Burn 3 time (sec) | 26.6 | 25.8 | | |

All Shuttle/Centaur G modeling data was taken or extrapolated from the Colt and mini-Colt, including electrical power, propellant loadings, residuals, boiloffs, and reaction control system (RCS) usage. Usages associated with the third burn were assumed to be the same as second burn usages (except for the second transfer orbit coast boiloff, which was estimated from the first transfer orbit coast based on time). Appendix A contains 2B and 3B Centaur propellant tanking information. Appendix B contains RL10A-3-3B engine modeling. Appendix C contains net payload calculations. Appendix D contains $LH_2$ boiloff and RCS usage modeling. Space Shuttle lift commitment varied from 60,500 lb at LAZ = 90° (i.e., parking orbit $i$ = 28.45°) to 43,900 lb at LAZ=35° (i.e., parking orbit $i$ = 57°) (Ref. 3). Note that Shuttle lift commitment included CISS + Orbiter supplied chargeables = ~ 9,267 lb (Ref. 3).

While the vehicle and mission were national defense-oriented, all data used and references discussed in this paper are unclassified. Further, no then-proprietary information was used. The Molniya mission

parameters are “generic” and were published as such in the open literature and unclassified documents of that time period. There is no mission peculiar information in this work.

# 3.0 Comparing 3B to 2B Transfers

## 3.1 Overview: How Orbital Elements Changed in 3B Versus 2B

A comparison of how the four orbital elements of interest (semi-major axis (a), radius of the perigee ($R_p$), inclination ($i$), argument of the perigee (ω)) changed throughout the mission for both the 2B and 3B transfers is shown in Figure 6. Though generally representative of the change in state conditions shown in Table 1 (columns 3 and 4), the specific values were based on data from the mini-Colt and Colt (Ref. 3 and 7), averaging the values from Main Engine Start (MES) and Main Engine Cut-Off (MECO) of each burn. Though the starting park orbits were similar, they differed significantly in inclination: 37° for 3B versus 57° for 2B. The reason for using these different parking orbit inclinations was to maximize launch vehicle performance for each transfer. As will be shown and explained in a later section, these maximized separated spacecraft weights at Molniya injection (despite a 20° parking orbit inclination difference) were almost the same. For that reason, the changes in elements on a percentage basis were plotted rather than absolute values in order to compare 3B to 2B. That is, 100 percent represents the total amount of change needed in a particular orbital element for 3B (or 2B) transfer from the park orbit to a Molniya orbit. One complication illustrated in Figure 6 was that some changes were not additively increasing. That is, some burns increased the values of certain elements beyond their final Molniya values, only to have a later burn reverse direction and reduce these values. These negative changes are represented graphically as overlaid fills in Figure 6. (For example: the ‘*a*’ change for the 3B transfer shows a narrow vertical bar for Burn 2 overlaid by the narrow horizontal bar of Burn 3, bringing the total bar down to 100 percent.) Similar reversals occur with Burns 2 and 3 for changes in $R_p$ for 3B, and also Burns 1 and 2 changes in ω for 2B. In addition, two of the stacked bars are significantly greater in percentage magnitude and thus extend beyond the given scale (243 percent for ω in 2B and 358 percent in $R_p$ in 3B). Their upper values are merely noted in Figure 6. The following description is given on the comparisons of the changes, with a detailed explanation of why the optimization changed the elements as it did from a physics and calculus perspective in a later section.

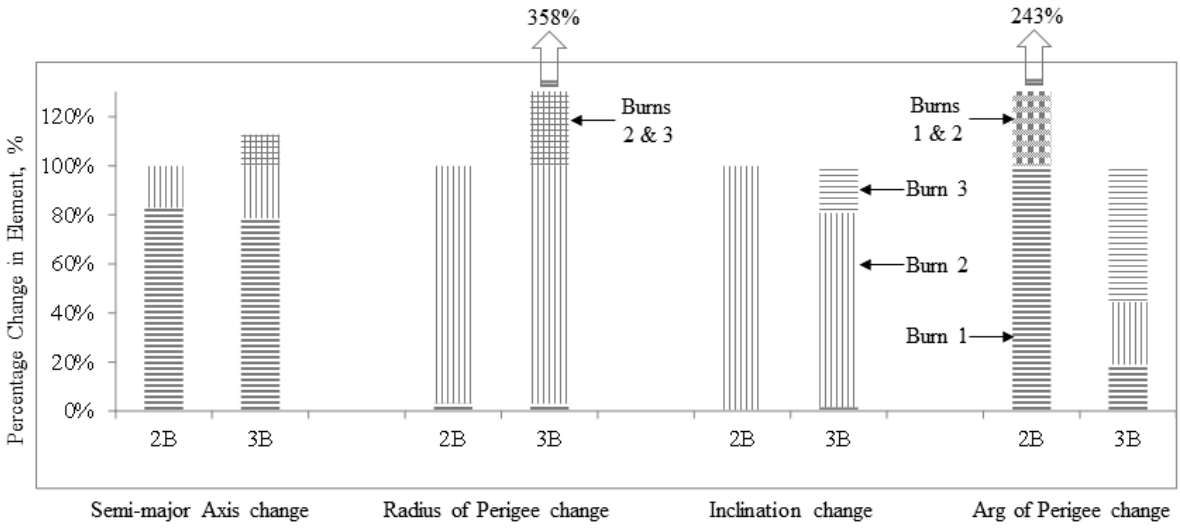


Figure 6.—Orbital Element Changes for Two and Three Burn Transfers.

The '*a*' was increased predominantly by Burn 1 in both the 2B and 3B transfers (columns 1 and 2 in Figure 6). While Burn 2 supplied a modest final increase in 2B, it greatly increased '*a*' by 3,674 nmi, which was well beyond its 100 percent value for the 3B transfer. This large of overshoot was unusual in trajectory design. Total orbital energy (which goes as the '*a*') almost always continually increases throughout a transfer until the final orbit (which is at the greatest total energy) is achieved. Indeed, a transfer orbit of greater orbital energy than the final orbit is almost always a case of 'wasting' performance and presumably non-optimal. As will be explained, a complex interaction existed between the optimized in- and out-of-plane steering, as well as the orbit element trade space, which was responsible for the existence of an optimal solution using a transfer orbit of greater energy than that the final orbit. This is illustrated in Figure 6 in the 3B bar, where Burn 2 is shown as a narrow vertical filled bar with Burn 3 overlaid as a narrow horizontal filled bar. The retrograde Burn 3 reduced the final value to 100 percent.

The $R_p$ was essentially unaffected by Burn 1 in 2B and 3B since the vehicle was at perigee (columns 3 and 4 in Figure 6). $R_p$ was raised solely by Burn 2 in the 2B transfer. For the 3B transfer, however, Burn 2 actually extended $R_p$ well off the scale of Figure 6 to a value of 358 percent (i.e., a 1,292 nmi increase in perigee altitude, a value of >3X the vertical scale of Figure 6). The retrograde Burn 3 then reduced the $R_p$ by 929 nmi, down to its 100 percent level. The reason for this overshoot is tied to the preceding discussion pertaining to '*a*'.

Figure 6 shows that the inclination change was done entirely by Burn 2 for 2B, while only 80 percent was done by Burn 2 for 3B (with Burn 3 doing almost all of the remaining change) (columns 5 and 6 in Figure 6). Burn 1 did negligible inclination change for either 2B and 3B since inclination change is a function of only out of plane thrust component and can be accomplished with less $\Delta V$ when applied at low orbital velocities (favoring high altitudes).

The $\omega$ change was considerably different in 2B versus 3B (columns 7 and 8 in Figure 6). It is important to first recognize that for a circular orbit, $\omega$ is undefined, and can change significantly for a near-circular orbit even with minor propulsive thrust. For 2B, Burn 1 changed $\omega$ well beyond (243 percent) the Molniya value (i.e., twice the vertical scale shown). Burn 2 then reversed this change and significantly brought $\omega$ to its final value. Note that Burn 1 is illustrated as thick horizontal fill, while Burn 2 is shown overlaid as thick vertical fill (unlike the other bars which show Burn 2 as thin vertical fill; a consequence of the limitations within the graphical software.) For 3B, $\omega$ was changed 20 and 25 percent during Burns 1 and 2, respectively, leaving the majority (55 percent) of the change for Burn 3.

To gain insight into why the optimization arrived at these solutions (Table 1 and Figure 6), the Centaur G steering angles, burn times, and time derivatives of the orbital elements (as functions of the steering angles) will be discussed. If all three of the angular components of thrust were known, they could be used with the time derivatives of the orbital elements to calculate the instantaneous change in each element to clarify the results of the optimization. While the archived trajectory output contained pitch and yaw steering angles (and their derivatives), these angles unfortunately were not calculated for the same coordinate system (for reasons lost to time). While the out of plane (yaw) steering data was in the orbital plane system, the pitch angle steering data was with respect to a local horizontal plane system. Thus in-trajectory-plane steering angle and their rates of change could not be used with the time derivative equations (discussed below), though their sign could be inferred. The out-of-trajectory-plane steering data however was available in the output files, so the yaw angle data is given in Table 2 and will be used in this assessment. Since the trajectories cannot be readily rerun, this paper must rely of what is available in the historic output files. The "*T*-*N*-*W*" coordinate system for these derivatives is a rotating reference frame centered at the Centaur/spacecraft within the instantaneous orbital plane. The *T* vector is tangent to the flight path and in the orbital plane. The *N* vector is normal to the flight path and also in-plane. The *W* vector is out of the orbital plane and positive when the acceleration is positive (i.e., in the direction of the angular momentum vector).

TABLE 2.—MAIN BURN STEERING CHARACTERISTICS

| | 3 Burn Aerospace PhD Thesis | 3 Burn NASA GRC | 3 Burn Aug 1984 mini-Colt | 2 Burn Oct 1985 Colt |
|---|---|---|---|---|
| Burn 1 of duration (sec) | 193.4 | 190.9 | 284.82 | 212.3 |
| MES-1 state | | | | |
| T and N angles (sign) | –3.1150 | –3.0148 | + and + | + and – |
| W angle (yaw) (deg) | 9.2430° | –9.1460° | –10.3800° | –5.2795° |
| W angle rate of change (deg/sec) | –0.0333 | 0.0330 | 0.0337 | 0.0364 |
| MECO-1 state | | | | |
| T and N angles (sign) | | | + and + | + and – |
| W angle (yaw) (deg) | | | –1.537° | 1.6530° |
| W angle rate of change (deg/sec) | | | 0.0268 | 0.0302 |
| Burn 2 of duration (sec) | 69.5 | 67.9 | 97.6 | 29.6 |
| MES-2 state | | | | |
| T and N angles (sign) | | | + and + | + and + |
| W angle (yaw) (deg) | | | 72.4570° | 64.8749° |
| W angle rate of change (deg/sec) | | | –0.0968 | –0.1562 |
| MECO-2 state | | | | |
| T and N angles (sign) | | | + and + | + and + |
| W angle (yaw) (deg) | | | 55.4149° | 59.6375° |
| W angle rate of change (deg/sec) | | | –0.0409 | –0.0365 |
| Burn 3 of duration (sec) | 26.6 | 25.8 | 27.0 | --- |
| MES-3 state | | | | |
| T and N angles (sign) | | | – and + | --- |
| W angle (yaw) (deg) | | | –53.4281° | --- |
| W angle rate of change (deg/sec) | | | –0.2703 | --- |
| MECO-3 state | | | | |
| T and N angles (sign) | | | – and + | --- |
| W angle (yaw) (deg) | | | –61.8898° | --- |
| W angle rate of change (deg/sec) | | | –0.0740 | --- |
| Thrust / weight (initial) | 1.0000 | 1.0074 | | |
| Thrust / weight (final) | 2.8045 | 2.8963 | | |
| Total $\Delta V$ (ft/sec) | 14930.16 | 14943.40 | | |
| Mass (final)/Mass (initial) | 0.3566 | 0.3457 | | |

The time derivatives of the orbital elements can be expressed as functions of the orbital elements themselves and components of the pertubative acceleration vector (i.e., thrust), in terms of in-plane and out of plane components. Equations (1) to (4) are the time derivatives for semi-major axis, radius of the perigee, inclination, and argument of the perigee, respectively (Ref. 11). Although the LEOs for the 3B and 2B transfers varied significantly in inclination (37° vs. 57°, respectively), meaningful comparisons between the two transfers can still be made by examining the solutions of Equations (1) to (4) and the corresponding steering angles (Table 2). Using the orbital element values from the trajectories based on data in the mini-Colt and Colt (consistent with the orbital data in Table 1), the coefficients for each thrust vector component were calculated for 3B and 2B using Equations (1) to (4), averaging the MES and MECO values. The results of these calculations appear in Table 3.

$$\frac{\partial a}{\partial t} = \left[\frac{2a^2 V}{\mu}\right] T \tag{1}$$

$$\frac{\partial R_p}{\partial t} = \frac{1}{V}\left\{\left[2R_p \frac{1-\cos\theta}{1+e}\right] T + \left[r\sin\theta\right] N\right\} \tag{2}$$

$$\frac{\partial i}{\partial t}\left[\frac{r}{\sqrt{l\mu}}\cos(\theta+\omega)\right] W \tag{3}$$

$$\frac{\partial \omega}{\partial t} = \frac{1}{V}\left\{\left[\frac{2\sin\theta}{e}\right] T + \frac{r}{le}\left(2e + \cos\theta + e^2\cos\theta\right) N - \left[\frac{rV}{\sqrt{l\mu}}\sin(\theta+\omega)\cot i\right] W\right\} \tag{4}$$

The values in Table 3 can be viewed as indicators of the relative ease of changing the orbital elements at particular points in orbits. As will be shown, the total vehicle performance of the 3B transfer was almost identical to that of the 2B transfer. Thus, the coefficients in Table 3 in the aggregate represent approximate equivalent difficulty paths leading to a comparable result (i.e., comparable mass to Molniya orbit). The combination of the Table 3 coefficients, the thrust component for each element, and the burn time can provide insight to the variationally-derived values in Figure 6. For example: the variationally-derived change in semi-major axis for Burn 1 in 3B transfer was 8,466 nmi. The rough approximation would be the combination of the Table 3 value (4,485 sec), the thrust component (0.00345 nmi/sec$^2$), and the burn time (285 sec), yielding 4,410 nmi. Thus, while this linear approximation of a non-linear burn is in error by a factor of two, it is still adequate to discuss general trends.

TABLE 3.—COEFFICIENTS OF ESTIMATED TIME DERIVATIVES OF ORBITAL ELEMENTS.

| | 3 Burn | | | 2 Burn | | |
|---|---|---|---|---|---|---|
| | T | N | W | T | N | W |
| Burn 1 | | | | | | |
| $\Delta a/\Delta t$ | 4,485 | --- | --- | 4,629 | --- | --- |
| $\Delta R_p/\Delta t$ | 1 | 34 | --- | 2 | -40 | --- |
| $\Delta i/\Delta t$ | --- | --- | –0.0595 | --- | --- | –0.0129 |
| $\Delta w/\Delta t$ | 0.0544 | 0.8351 | 0.2594 | –0.0630 | 0.8112 | 0.1331 |
| Burn 2 | | | | | | |
| $\Delta a/\Delta t$ | 11,004 | --- | --- | 13,183 | --- | --- |
| $\Delta R_p/\Delta t$ | 4,796 | 5,564 | --- | 3,095 | 4,011 | --- |
| $\Delta i/\Delta t$ | --- | --- | 0.5707 | --- | --- | 0.4649 |
| $\Delta w/\Delta t$ | 1.1331 | 0.5318 | –0.3068 | 0.9600 | 0.5525 | –0.1932 |
| Burn 3 | | | | | | |
| $\Delta a/\Delta t$ | 11,882 | --- | --- | --- | --- | --- |
| $\Delta R_p/\Delta t$ | 5,491 | –6,402 | --- | --- | --- | --- |
| $\Delta i/\Delta t$ | --- | --- | –0.4276 | --- | --- | --- |
| $\Delta w/\Delta t$ | –1.1184 | 0.5142 | –0.3389 | --- | --- | --- |

## 3.2 The 3B Transfer

The first burn ("Burn 1") was 285 sec long and was 70 percent of the sum of the three orbital burn times. Burn 1 was essentially planar and occurred well into the third quadrant of the argument of the latitude (u); that is, just before the southern antinode. It primarily increased the orbital energy (thus '*a*', thus the period). It also generally fixed the perigee, and likewise the ω of the final orbit. Burn 1 was largely within the orbital plane and raised apogee altitude to ~17,059 nmi (~80 percent of Molniya apogee altitude of 21,295 nmi). The burn also rotated the ω to 253°, only 17° short of Molniya's 270°. (Note: ω value does not correspond to park orbit in Table 1 due to rapidly changing near-zero eccentricity early in the finite burn.) The *i* and $R_p$ were almost totally unchanged from that of the parking orbit. The first transfer orbit extended from 10.5° to 143.4° of true anomaly (θ) and was 1.6 hr in duration.

The Burn 1 coefficients of the perturbations (Eq. (1) to (4)) appear in Table 3. The coefficient for the semi-major axis (*a*) derivative (Eq. (1)) was positive (4,485 sec), and since the optimization showed a large increase in '*a*', then the in-plane thrust component *T* must be large and positive. The coefficients in the $R_p$ derivative were de minimis (Eq. (2)) since Burn 1 took place at perigee. The combination of the small negative coefficient for the inclination (*i*) derivative of –0.0595sec/nmi (Eq. (3)) and the small negative (–10.4° at MES and –1.5° at MECO) out of plane thrust component *W* (Table 2) illustrated why almost no plane change was performed in Burn 1. Since *W* was negative and the out of plane coefficient for ω was positive (0.2594 sec/nmi), its product was negative. Since ω increased, then the in-plane thrust component *N* must also be positive in order for its combination with its larger coefficient (0.8351 sec/nmi) to be greater than that of the out on plane combination. (The coefficient of *T* was smaller (0.0544 sec/nmi) than that of *N*, yielding a combination likely to be smaller.) Note that the in-plane coefficients were all positive, while the out of plane coefficients (*i* and ω) were of differing sign. Thus, out-of-plane thrust driven changes in *i* and ω would be at cross purposes.

The second burn (Burn 2) was 98 sec in duration. It occurred in the first quadrant of '*u*'; that is, just after the node. Burn 2 was significantly both in- and out-of-plane, raising $R_p$ considerably and further increasing '*a*', while at the same time increasing '*i*'. The '*a*' was increased by 3,674 nmi to a value of 15,713 nmi (which was 1,375 nmi greater than Molniya). This corresponded to a perigee increased to 1,434 nmi altitude (alt) from the first transfer orbit (~142 nmi alt), and an apogee increased to 23,116 nmi alt (1,821 nmi higher than Molniya orbit apogee of 21,295 nmi alt). This is one of the most remarkable aspects of the 3B solution, since orbit-to-orbit transfers almost always increase in total energy (which is directly proportional to semi-major axis) until the final orbit is reached. The inclination was greatly increased from the first transfer orbit of 37.5° to the second transfer orbit of 58.3°. The ω was increased 5.5° to a value of 258.2°. The second transfer orbit extended from 127° to 224° of θ and was 10.1 hr in duration.

The Burn 2 coefficients of the perturbations were quite different than those of Burn 1. The coefficient for the '*a*' derivative (Eq. (1)) was large and positive (11,004 sec; Table 3), and since the optimization showed an increasing '*a*', then the in-plane thrust component *T* must be positive. The $R_p$ coefficients were also both large and positive (4,796 and 5,564 sec for *T* and *N*, respectively; Table 3), and since $R_p$ had to be raised, both in-plane thrust components *T* and *N* were positive. The combination of the large positive coefficient for the inclination derivative of 0.5707 sec/nmi (Table 3) and the large positive (72.5° at MES and 55.4° at MECO; Table 2) out of plane steering component illustrate why the large plane change of 21° was possible. The ω increase was due to the sum of the combinations of the large, positive in-plane perturbation coefficients (1.1331 and 0.5318 sec/nmi) (Eq. (4)) and in-plane thrust components being greater than the out of plane combination with the coefficient –0.3068 sec/nmi. Similar to Burn 1, in Burn 2, the in-plane coefficients were all positive, while the out of plane coefficients (*i* and ω) were of differing sign. Thus, out-of-plane thrust driven changes in *i* and ω would be at cross purposes.

The third burn (Burn 3) was the shortest at 27 sec duration. It occurred in the second quadrant of '*u*'; that is, approaching the descending node. (An oddity of the solution is that Burn 3 was located in the general vicinity of the alternate second burn location for a 2B transfer.) Like Burn 2, Burn 3 was also significantly both in- and out-of-plane. However, Burn 3 was retrograde. It performed the majority of the ω change (~12°) while also reducing '*a*' (by 1,375 nmi) and $R_p$ (by 929 nmi) to their Molniya values. A modest amount of plane change was also performed (5°). True anomaly at injection was 217.0°.

Burn 3 coefficients of the perturbations (Table 3) were quite different than those of Burns 1 or 2, both in sign and magnitude. The coefficient of '*a*' derivative (Eq. (1)) was very large and positive (11,882 sec), and since the optimization showed a decreasing '*a*', then the in-plane thrust component *T* had to be negative. The $R_p$ coefficients were also both large (5,491 and –6,402 sec for *T* and *N*, respectively; Eq. (2)), and since $R_p$ had to be lowered, in-plane thrust component *N* was most likely positive, while T is indeterminate (though likely negative). The combination of the moderate coefficient for the inclination derivative (Eq. (3)) of –0.4276 sec/nmi and the large negative (–53.4° at MES and –61.9° at MECO) out of plane steering component for Burn 3 (Table 2) enabled the modest positive plane change. The considerable negative out of plane component *W* together with the ω coefficient in Table 3 of –0.3389 sec/nmi (Eq. (4)) yielded a positive value, which was also true of the (likely) negative value of the in-plane component *T* taken with its coefficient –1.1184 sec/nmi. The positive in-plane component *N* with its Table 3 ω coefficient 0.5142 sec/nmi also yielded a positive value. Unlike Burn 2, in Burn 3, the in-plane coefficients were of varying sign, while the out of plane coefficients (*i* and ω) were both negative. Thus, the negative out-of-plane thrust driven changes in *i* and ω had the effect of increasing both inclination and ω.

### 3.3 The 2B Transfer

Burn 1 was 212 sec long and was 88 percent of the sum of the two orbital burn times. Like the 3B transfer, Burn 1 was essentially planar and occurred well into the third quadrant of the argument of the latitude (*u*); that is, just before the southern antinode. It primarily increased the orbital energy (thus '*a*', thus the period). It also generally fixed the perigee, and likewise the ω of the final orbit. Burn 1 was largely within the orbital plane and raised apogee altitude to 17,954 nmi (~84 percent of Molniya apogee altitude of 21,295 nmi). The burn also reduced the ω to 266°, slightly overshooting the Molniya value, leaving it 4° short of Molniya's 270°. (Note: ω value does not correspond to park orbit in Table 1 due to rapidly changing near-zero eccentricity early in the finite burn.) The *i* and $R_p$ were almost totally unchanged from the parking orbit. The transfer orbit extended from 8.2° to 130.8° of true anomaly (θ) and was 68 min in duration.

Burn 1 coefficients of the perturbations (Eq. (1) to (4)) for the 2B transfer also appear in Table 3 and were very similar (both in magnitude and sign) to those of the 3B transfer. The coefficient for the '*a*' derivative (Eq. (1)) was positive (4,629 sec), and since the optimization showed an increasing '*a*', then the in-plane thrust component T must be large and positive. Similar to the 3B case, the coefficients in the $R_p$ derivative (Eq. (2)) were de minimis since Burn 1 took place at perigee. The combination of the small negative coefficient for the '*i*' derivative (Eq. (3)) of –0.0129sec/nmi and the small, mostly negative (–5.3° at MES and 1.6° at MECO) out of plane thrust component W (Table 2) illustrated why almost no plane change was performed in Burn 1 for the 2B transfer. Since *W* was mostly negative and the out of plane coefficient was positive, its combination was negative. Since ω decreased, overshooting its final Molniya value, then in-plane thrust components *T* and *N* were most likely positive (where $T > N$) in order for the sum of the combinations to be less than that of the out-of-plane combination. (The coefficient of *T* was likely larger than *N* since the burn was primarily an orbit raising maneuver. Further, the *T* coefficient (-0.0630 sec/nmi) was smaller than the N coefficient (0.8112 sec/nmi).) Note that the in-plane coefficients were not all positive, though small angle averages were the real reason for this occurrence. The out of

plane coefficients (*i* and ω), like in the case of 3B, were of opposite sign, thus, changes in i and ω would be at cross purposes. This set up a major difference between 2B and 3B. Since the i and ω coefficients were of opposite sign in both Burn 1 and 2, and inclination had to be changed in Burn 2, this forced most of the ω change into Burn 1. Indeed, the ω change had to overshoot the target value of 270° in order to enable the positive change for inclination.

Burn 2 was 30 sec in duration. It occurred in the first quadrant of '*u*'; that is, just after the node. Burn 2 was significantly both in- and out-of-plane, raising all elements to their Molniya values. '*a*' was increased by 1,849 nmi to a Molniya value of 14,335 nmi. The $R_p$ was increased 360 nmi to a Molniya orbit perigee of 502 nmi alt. The inclination was increased 6.4° to a final Molniya value of 63.4°. The ω was increased 3.8° to a Molniya value of 270°. True anomaly at injection was 124.9°.

Burn 2 coefficients of the perturbations (Table 2) for 2B transfer were similar to those of the 3B transfer in terms of sign and magnitude. The coefficient for the semi-major axis (*a*) derivative (Eq. (1)) was very large and positive (13,183 sec), and since the optimization showed an increasing '*a*', then the in-plane thrust component *T* must be positive. The $R_p$ coefficients were also both large and positive (3,095 and 4,011 sec for *T* and *N*, respectively; Eq. (2)), and since $R_p$ had to be raised, both in-plane thrust components *T* and *N* were positive. The combination of the positive coefficient for the inclination derivative (Eq. (3)) of 0.4649 sec/nmi and the positive (64.9° at MES and 59.6° at MECO) out of plane steering component illustrate why the entire plane change was performed by Burn 2. The considerable positive out-of-plane steering component *W* together with its coefficient of –0.1932 sec/nmi (Eq. (4)) yielded a negative value, which suggested that one or both of the in-plane components *T* and *N* were sufficiently positive to produce a sum of their combinations (with their coefficients 0.9600 and 0.5525 sec/nmi, respectively) that was greater than that of the out-of-plane combination.

### 3.4 Summary Observations: 3B Versus 2B

Several observations can be made pertaining to the existence of an optimal three burn transfer which yielded almost identical performance as a two burn transfer, despite the considerable additional inclination change performed (20°). Comparing 3B to 2B orbital element derivative coefficients for each burn provided insight as to why it was desirable to increase both the '*a*' and $R_p$ well beyond their final requirements, only to reduce them back down after changes were made in both *i* and ω.

The magnitudes of each of the derivative coefficients in Burn 1 for both 3B and 2B were comparable, as were their signs (with some exceptions for those of small absolute values). The 3B and 2B coefficients for '*a*' were almost the same and produced similar results. This was consistent with the expectation that Burn 1 was primarily an apogee raising maneuver ($R_p$ change was approximately zero since the Burn 1 was at perigee, reflected by de minimus coefficients). The coefficients for inclination were also small and comparable for both 3B and 2B, producing almost no plane change since it was not optimal to do so at high speed (i.e., at perigee). The 3B and 2B coefficients for ω were roughly comparable in magnitude, but with a difference in sign for T. Although the percentage change in ω was large in 2B (Figure 6), the actual value (like all ω changes) was small (~ 6½°). The range in thrust components was similar in magnitude and sign. Although the burn time for 3B was ⅓ greater than that for 2B (285 vs. 212 sec, respectively), with somewhat similar thrust angles, it did not produce greater changes in the orbital elements compared to the 2B transfer. Thus with the exception of the large percentage changes in ω, the changes in the other orbital elements done by Burn 1 in 3B and 2B were similar (as illustrated in Figure 6).

Unlike Burn 1, the magnitudes of each of the Burn 2 derivative coefficients for 3B and 2B were noticeably different. The 2B '*a*' value was surprisingly greater than the 3B value, despite the fact that the 3B increase in '*a*' was proportionately larger than 2B's. This greater increase in '*a*' was due largely by the 3B Burn 2 time which was triple that of 2B's Burn 2 (~98 vs. ~30 sec). Nevertheless, the change in

‘*a*’ in 2B was facilitated by its larger coefficient (13,183 vs. 11,004 sec). Also note that the coefficients for ‘*a*’ for both 3B and 2B were nearly triple their Burn 1values. The 2B coefficients for $R_p$ were ~ ⅔ of the value of the 3B coefficients. Combined with the triple burn time, the 3B $R_p$ coefficients illustrated the greater ease in $R_p$ increase (Figure 6). The inclination coefficient was greater for 3B (keeping in mind that the units are radians/sec). It was this greater inclination coefficient and splitting up the plane change between Burns 2 and 3 in the 3B solution, which led in large part to the existence of a three burn solution to Molniya orbit. Though all of the plane change in 2B was done in Burn 2, while only 80 percent was done in 3B, the absolute values of these changes were 6.4° versus 21°, respectively. (Later, it will be shown that requiring a large change in inclination (i.e., a lower inclination parking orbit) was fundamental to the very existence of a three burn transfer.) While the ω coefficients were slightly more favorable for the 3B transfer, the 2B percentage change in ω was large, though the absolute value of the ω change in 3B was greater. The thrust components’ magnitudes and signs were comparable for 2B and 3B.

Burn 3 was largely to complete the inclination and ω change, while subtracting out the excess ‘*a*’ and $R_p$ altitude. The ‘*a*’ coefficient was greater (i.e., more favorable) for Burn 3 than it was in Burn 2. The same was also true of the $R_p$ coefficients, which were also greater that their absolute values in Burn 2. The inclination coefficient was smaller than that in Burn 2, but still significant to enable the remaining 5° plane change. The ω coefficients were comparable to those in Burn 2, enabling the remaining significant change in ω to its final value. It was also interesting to compare 3B’s Burn 3 coefficients to those of 2B’s Burn 2. While the ‘*a*’ coefficients were almost comparable, the $R_p$ coefficients for 3B were significantly greater. Three B’s inclination coefficient was slightly lower than that of 2B, while 3B’s ω coefficients were greater. All of this suggests that the orbital element space of 3B’s Burn 3 was generally more attractive than those of 2B’s Burn 2.

But it was the ω coefficients which implied why it was advantageous to incur these two losses: because the thrust component *T* was negative while its coefficient is large and negative (yielding a positive combination). Similarly, both the *N* and *W* components yielded positive combinations. Thus the entire ω derivative yielded a significant positive sum (unlike in Burn 2). Further, compared to 2B’s Burn 2 case, even though the burn times were almost the same, the coefficients did not complement, but competed, producing a much smaller change in ω in absolute terms.

Why an optimal 3B solution existed despite greater propellant usage and an intermediate transfer orbit with greater energy than the final orbit was apparent by observing that:

- Element derivative coefficients for 3B’s Burns 2 and 3 were mostly greater than 2B’s Burn 2
- Orbital element change-spaces for 3B were more Δ*V*-efficient in the aggregate
- Splitting up changes into Burns 2 and 3 enabled more optimal changes
- Yaw derivative coefficients were of opposite sign for *i* and ω in 2B, forcing costly ω changes into Burn 1 (where instead, 3B could defer them into Burn 3)
- Derivative for ω was a function of both in- and out-of plane thrust components (coupling effects)
- Significant change in ‘*i*’ was necessary for existence of 3B solution (see next section)
- Derivative coefficients in 3B’s Burn 3 in-plane elements were opposite in sign, enabling retrograde burns be done to subtract out excess *a* and $R_p$, still enabling large changes in *i* and ω

In summary: the 3B transfer with comparable performance existed because it was more advantageous to split up and perform the ‘*i*’ and ω changes in more favorable orbital element spaces even though it cost performance to temporarily increase ‘*a*’ and $R_p$ beyond their required Molniya values (and eventually subtract them back out).

# 4.0 Variation with Parking Orbit Inclination

## 4.1 Three Burn Transfer as a Function of Parking Orbit Inclination

An analysis was performed on how the 3B transfer changed as parking orbit inclination was varied. As was discussed earlier, the inclination was increased primarily by Burn 2 for 3B transfers. As the park orbit inclination was increased from 28.45° and total plane change required decreased, most of the reduced plane change continued to take place in Burn 2. Figure 7 illustrates the change in Transfer Orbit 2's inclination. The regions labeled represent the amount of plane change done by Burns 2 and 3. The amount performed by Burn 3 also decreased but at a much smaller rate. Eventually a point was reached where the amount of plane change was small enough that it could be done entirely by Burn 2, with minimal adverse effect on argument of the perigee. At an inclination of 57°, Burn 3 went to zero, the 3B solution vanished and the 3B transfer degenerated into the 2B solution. It is of academic interest to note that Burn 2 could be made to vanish instead, whereby Burn 3 would become the second burn at 57°. This alternate 2B transfer, however, would not be desirable in lieu of the standard 2B transfer due to its longer transfer time. Beyond 57°, only the 2B solution exists. As the parking orbit inclination continued to increase, approaching the Molniya value (63.4°), the 2B trajectory reduced to a planar Holman transfer.

The data pertaining to the change in $R_p$ altitude as a function of park orbit inclination was not archived in the original analysis. However, the change in radius of apogee ($R_a$) altitude for 3B transfer was tabulated and was plotted in Figure 8. $R_a$ was seen to significantly decrease with increasing park orbit inclination and had a minimum at 54° inclination. At a park orbit inclination of 57° and above (where the 3B solution vanished) $R_a$ altitude became that of Molniya's (21,295 nmi). As was discussed earlier, the majority of the ω change was done by Burn 3 for the 3B transfer. As the park orbit inclination was increased from 28.45°, the total ω change required decreased. Most of the reduction in ω change came from Burn 3, with the amount performed in Burn 2 remarkably constant. Figure 9 showed the change in Transfer Orbit 1 and 2's argument of the perigee. The regions labeled therefore represent the amount of ω change done by Burns 2 and 3. At a park orbit inclination of 57° and above (where the 3B solution vanished) the remaining ω change was performed solely by Burn 2. The Burn 1 values for ω were not retained from the original analysis.

The change in semi-major axis as a function of park orbit inclination was not archived in the original analysis. However, the change in $C_3$ (orbital energy per unit mass (an analogous quantity)) was tabulated and plotted in Figure 10. Burn 2 was seen to increase $\Delta C_3$ until a maximum was reached at an inclination of 36°. It then steadily decreased until a parking orbit of 57°, where the $\Delta C_3$ went to zero for Burn 3, greatly reducing the need for large increases in $C_3$ by Burn 2 (thus the change in slope by Burn 2). Burn 3 was always retrograde (i.e., decreased $C_3$) throughout the 3B range of inclinations. As will be discussed in the next section, the maximum which occurred in Burn 2 corresponded to the point where Centaur propellants had to be off-loaded in order to satisfy decreasing Shuttle lift capability (as LAZ decreased to increase park orbit inclination). Thus the $\Delta C_3$ of Transfer Orbit 2 had to decrease above a park orbit inclination of 36°.

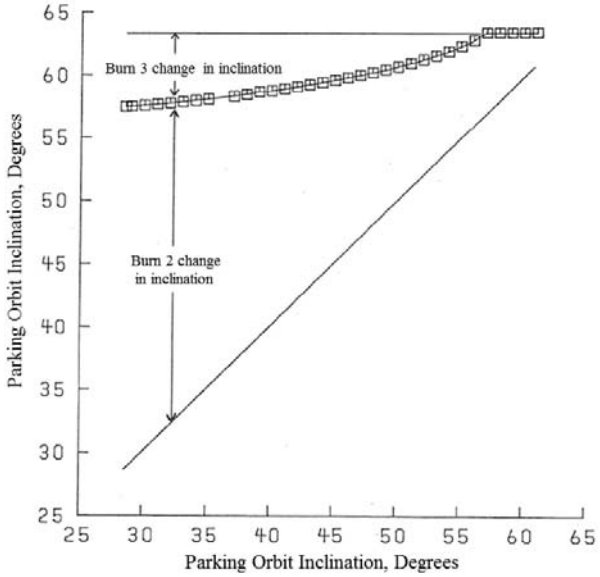


Figure 7.—Plane Change Versus Park Orbit Inclination for 3B Transfer

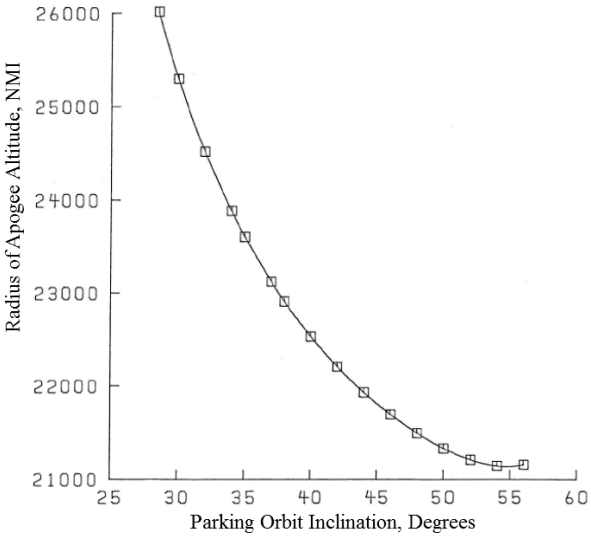


Figure 8.—Apogee Radius Change Versus Park Orbit Inclination for 3B Transfer

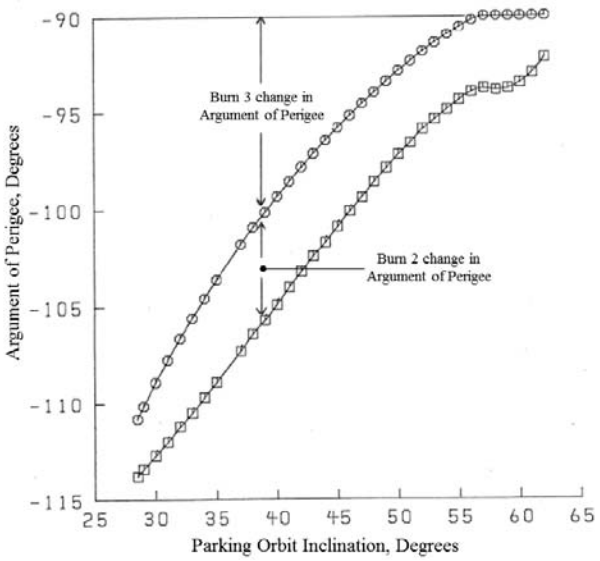


Figure 9.—Argument of Perigee Versus Park Orbit Inclination

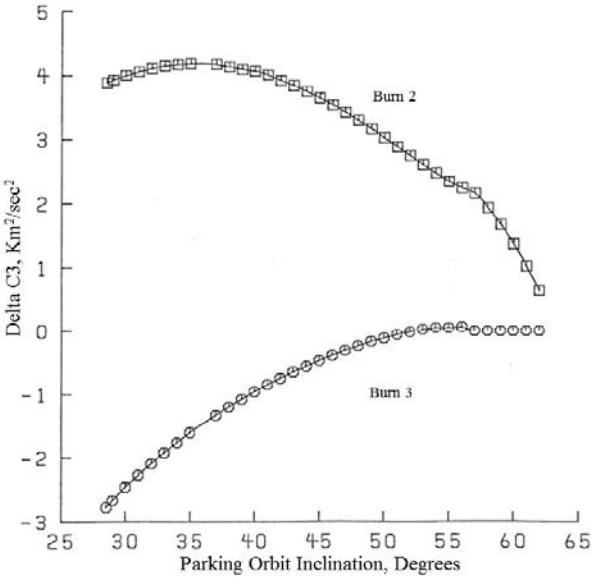


Figure 10.—Change in $C_3$ Versus Park Orbit Inclination

## 4.2 Performance Versus Park Orbit Inclination for 3B Versus 2B

An analysis was performed of the variation of certain orbital characteristics for 3B and 2B transfers as a function of parking orbit inclination. This was done to determine total vehicle performance (including identifying the optimum park orbit inclination), understand the orbital mechanics, and begin to determine if there were any mission-driven impacts on vehicle systems. Thirty-four trajectories were run for parking orbit inclinations between 28.5° and 62°.

In order to calculate net separated spacecraft mass (payload) as a function of inclination for both 3B and 2B, two quantities had to be calculated: the “wet Centaur” mass (which included propellant margins

and residuals) for 3B and 2B (both fully loaded and off-loaded) and the Shuttle lift capability—both as a function of park orbit inclination. The wet Centaur tabulation appears in Appendix C. The Shuttle lift capability and its impact on Centaur propellant off-loading and propulsion operation were calculated as follows:

The "Space Shuttle lift commitment" varied from 60,500 lb at LAZ = 90° (i.e., parking orbit $i$ = 28.45°) to 43,900 lb at LAZ=35° (i.e., parking orbit $i$ = 57°) (Ref. 3). (Note that Shuttle lift commitment included CISS + Orbiter supplied chargeables = ~ 9,267 lb) (Ref. 3). These values were consistent (and slightly conservative) with the "Space Shuttle lift capability" analysis which illustrated that at park orbit inclination of 57°, the Shuttle capability was 45,400 lb (Ref. 12). For every 1° increase in park orbit inclination, the Shuttle lift commitment decreased by 581 lb. At the lower inclinations where the Centaur was fully tanked, every 1° increase meant an increase in total stack performance of approximately 285 lb. From 28.45° to approximately 35.75°, the oxidizer-to-fuel ratio ('o/f') equaled 6.1579 and was held constant. This was done for simulation purposes only and did not reflect how the propellant utilization system would actually operate. At 35.75°, the Shuttle lift commitment equaled the combined weight of a fully loaded Centaur and a maximized payload. Beyond that point, $LO_2$ would be offloaded until the o/f ratio reached 6.0. This region (~1° wide) was not simulated. Starting at 36.75° and continuing up to 62.0°, both $LO_2$ and $LH_2$ were offloaded to maintain a 6:1 mixture ratio. The 2B fuel loading was modeled in a similar manner. All other modeling was unchanged from the baseline. Appendix A and Appendix B contain the detailed explanation of propellant loading and the concomitant engine modeling.

For the fully loaded region, the same "wet Centaur" weight (i.e., Centaur including residuals and propellant margins) was subtracted from the 3B and 2B burnout weights. Likewise, a wet Centaur weight characteristic of an offloaded mission was used for the higher inclination transfers. By plotting maximum payload (i.e., jettison weight – wet Centaur) , a one to one comparison could be made between 3B and 2B for a particular inclination. In addition, it allowed the different residuals and reserves associated with full tanked and offload missions to be taken into account. Appendix C contains net payload calculations. Appendix D describes $LH_2$ boiloff and RCS usage.

Figure 11 summarizes the results of 3B versus 2B performance versus parking orbit inclination. Performance rapidly increased with inclination as excess Shuttle lift capability was traded for more Shuttle supplied plane change. The knees of the curves correspond to where the Shuttle lift capability (as a function of park orbit inclination) equaled the fully tanked Centaur + payload weight. Centaur offloading started at the knee of each curve (~37° for 3B, ~38° for 2B). As the park orbit inclination increased further, total system performance leveled off for 3B, then slowly decreased. For 2B however, performance continued to gradually increase, reaching a maximum of 9,682 lb at 51°. (While that was 130 lb greater than the 2B baseline at $i$ = 57°, it was decided earlier in the program not to go through the process of establishing a new Shuttle ascent profile. This decision preceded (and was independent of) the 3B to Molniya assessment.) Nevertheless, 3B had better performance than 2B up to a park orbit inclination of 44°. The 37° case represents the peak performance for 3B. Its payload of 9,545 lb was only 7 lb less than the 57° case for 2B (which was the baseline ascent for the 2B transfer). If launched into a 37° parking orbit, 3B performance would be comparable to 2B, but would be fully tanked. This was a major finding of the analysis and satisfied a primary goal of the study.

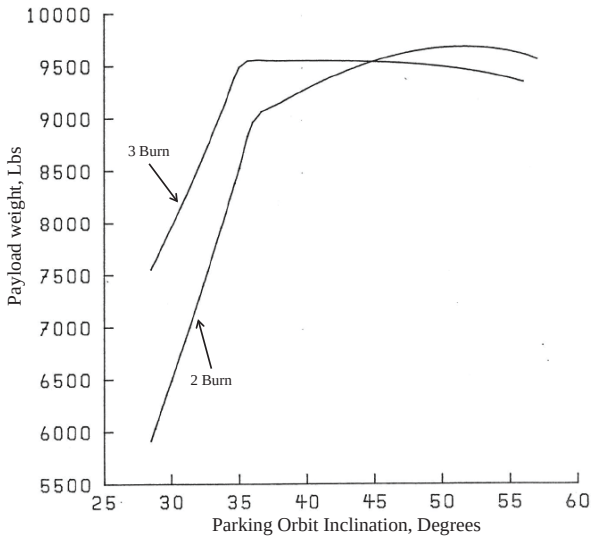


Figure 11.—Performance Versus Park Orbit Inclination for 3B and 2B Transfers

The performance curves did not coincide at 57° because of the losses associated with the settling phases. As the steady state main impulse went to zero, the fixed settlings, pre-chills, and RCS usages represented reductions in burnout weight that produced little ΔV in return. The effects of these losses associated with Burns 2 and 3 could also be estimated by approximating them as drop masses in the integrated trajectory optimization (see Appendix E). For Burn 3 in 3B ($i$ = 37°), each pound of propellant for settling took the place of 0.9 lb of payload. The rocket was in effect carrying dead weight through all of the burns, only to throw it away just before it reached the final orbit. These non-main impulse propellants amounted to well over 200 lb of lost performance. As Burn 3 went to zero (at $i$ = 57°), the two partials representing the Burn 2 and 3 transients became –0.9 and –1.0 in the limit, respectively. It was because 3B had this additional set of settling losses that its performance decreased singularly following the start of offloading, despite the smaller plane changes. The 2B performance continued to benefit from the shrinking plane changes until its second burn became short enough. Then it too began to suffer the same way as 3B.

The variation in duration of Burns 1, 2, and 3 for the 3B transfer are given in Figure 12. Burn 1 was the longest throughout the range of park orbit inclinations and varied between 282 to 217 sec. It was followed by Burn 2 which ranged between 101 and 32 sec. Burn 3 was 35 sec long at 28.45° and then vanished at 57°. Note that while Burn 1 had a slight maximum at 35° corresponding to the aforementioned onset of Centaur off-loading, Burn 2's slight maximum (~1 sec) took place a 32° (explanation unknown). The variation of Burns 1 and 2 for the 2B transfer are given in Figure 13. Again, Burn 1 was the longest throughout the range of park orbit inclinations and varied between 260 to 214 sec. Burn 2 steadily decreased, ranging between 194 and 30 sec; a much greater variation than in the case of 3B. Note that Burn 1 similarly had a modest maximum at 37° corresponding to the aforementioned start of Centaur off-loading. Note that the 57°case in 2B also represented the asymptotic 3B transfer at that same inclination.

The total "mission elapse times" (MET), which spanned from MES-1 to MECO-3 for 3B, as a function of park orbit inclination were plotted in Figure 14. The total times ranged from over 14 hr at 28.45° to 10.5 hr at 56°. The overall shape of the curve and the minimum at 54° inclination are coincident with the change in $R_a$ altitude for Burn 2 (Figure 8). The total MET for 2B (MES-1 to MECO-2) as a function of park orbit inclination were plotted in Figure 15. The times increased almost linearly from over 64 min at 28.45° to 77 min at 57°. This order of magnitude increase in MET for 3B versus 2B represented a major disadvantage for 3B, as more consumables would be needed to perform 3B transfers compared to 2B. The following discussion explains how the need for more consumables could be mitigated with modest changes to the Centaur vehicle.

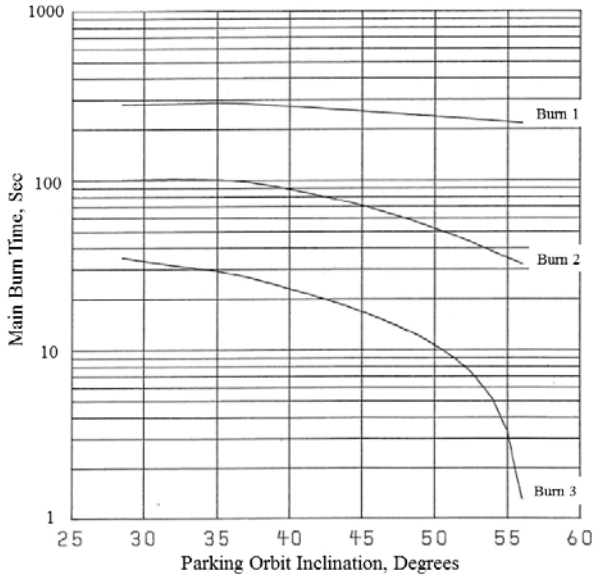


Figure 12.—Main Burn Times Versus Park Orbit Inclination for 3B Transfer.

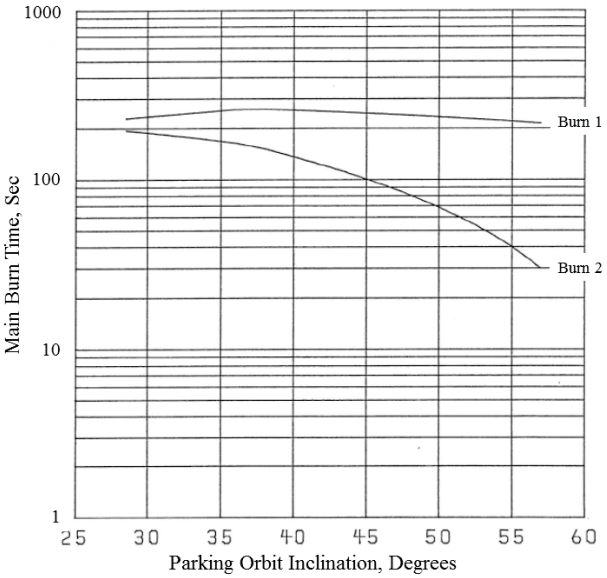


Figure 13.—Main Burn Times Versus Park Orbit Inclination for 2B Transfer.

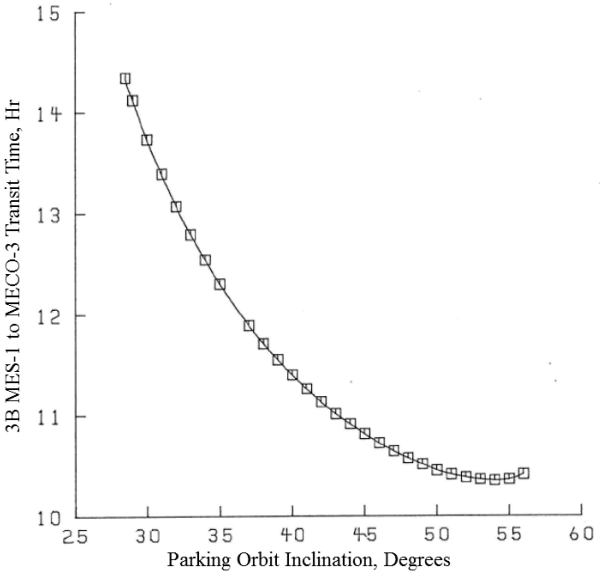


Figure 14.—Mission Elapse Time Versus Park Orbit Inclination for 3B Transfer.

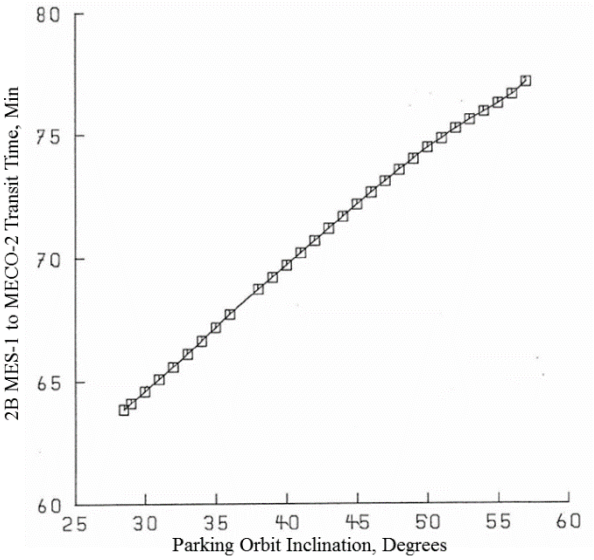


Figure 15.—Mission Elapse Time Versus Park Orbit Inclination for 2B Transfer.

## 4.3 Other Consumables (Electrical Power, $N_2H_4$, He)

A major concern of the 3B transfer was the long MET (12 hr at $i$ = 37°), driven largely by the second transfer orbit. Additional electrical power would be necessary to keep the stage alive. The standard Shuttle/Centaur G battery complement was three 250 A-hr batteries. At a typical 80 A average current usage, they provided enough power for only 9 hr, short of the needs for a 3B Molniya transfer. One solution to this shortfall was to use two of the three optional 150 A-hr payload batteries available on the G vehicle. Though intended for the payload, mission peculiar hardware could have been added to use them for Centaur instead in order to accommodate the longer duration 3B mission. Table 4 shows the estimated power requirements for a 3B Molniya mission. Electrical power usage (per unit time) by Centaur was roughly equally split between

avionics and fluid control, with the latter varying meaningfully depending on whether the propulsion system was in a coast, transient, or main burn phase (Ref. 13). Thus, duration was the primary driver of total power requirements. Using the standard complement of three Centaur batteries augmented by two payload batteries, a total 1050 A-hr was available to satisfy the calculated 943 A-hr required for a 3B mission starting from a 37° park orbit. The additional weight hit would be significant: 170 lb of batteries and ~ 30 lb for miscellaneous power transfer unit hardware and harnessing.

Two other consumables were also evaluated: hydrazine ($N_2H_4$) and helium (He). The standard Molniya mission loading of $N_2H_4$ monopropellant for the reaction control engines were 2 bottles (which included a 117 lb unallocated reserve). This was ample reserve to accommodate the additional 79 lb of $N_2H_4$ required for Transfer Orbit 2 (Table 5 and Appendix D) (Refs. 5 and 7). Regarding helium usage, the standard He pressurent loading were 2 large and 1 small bottle, for a total of 24 lb (which included a 5½ lb unallocated reserve). The additional He needed for Transfer Orbit 2 and Burn 3 usage was almost 9 lb. This could have been accommodated by replacing the small He bottle with a large bottle, which would satisfy the He usage while still maintaining a small (~1¼ lb) margin (Table 5). (Refs. 3 and 5) So the increased usage of both of these consumables could be accommodated with only modest system impacts. The additional net weight hit would be ~10 lb (for the larger He tank).

TABLE 4.—POWER REQUIREMENTS FOR 3B TRANSFER

| | Total | | | Load, A | Required, A-hr |
|---|---|---|---|---|---|
| | sec | sec | hr | | |
| Coasts | | 43045 | 11.957 | 76.5 | 914.7 |
| Transfer orbit 1 | 5361 | | | | |
| Transfer orbit 2 | 35884 | | | | |
| Post MECO-3 | 1800 | | | | |
| Burns | | 409 | 0.114 | 93.0 | 10.6 |
| Burn 1 | 285 | | | | |
| Burn 2 | 98 | | | | |
| Burn 3 | 26 | | | | |
| Transients (3) | | 750 | 0.208 | 83.0 | 17.3 |
| Total requirement | | 44204 | 12.279 | | 942.6 |
| Total capability of 3 Centaur + 2 payload batteries | | | | | 1050.0 |

TABLE 5.—HYDRAZINE AND HELIUM USAGE

| | $N_2H_4$ 2 Burn, lb | $N_2H_4$ 3 Burn, lb | He 2 Burn, lb | He 3 Burn, lb |
|---|---|---|---|---|
| Pre-MES-1 usage | 44 | 44 | 1.60 | 1.60 |
| Burn 1 | | | 7.34 | 7.34 |
| Transfer orbit 1 | 79 | 79 | 0.25 | 0.25 |
| Burn 2 | | | 8.73 | 8.73 |
| Transfer orbit 2 | 0 | 79 | 0 | 0.25 |
| Burn 3 | | | 0 | 8.73 |
| Post last MECO | 13 | 13 | 0.63 | 0.63 |
| Collision, contamination avoid | 49 | 49 | 0 | 0 |
| Dispersions/residuals/errors | 38 | 38 | 0 | 0 |
| Unallocated reserve | 117 | 38 | 5.45 | 1.27 |
| Total | 340 | 340 | 24.00 | 28.80 |
| $N_2H_4$ bottle (170 lb) | 2 | 2 | | |
| He bottle (large) | | | 2 | 3 |
| He bottle (small) | | | 1 | 0 |

# 5.0 Launch Windows

An analysis was done on the performance penalties associated with generating launch windows and deployment on later revolutions. This was done by having Centaur compensate for the orbit's nodal shift due to the Earth's rotation due to early or late launch, and/or the regression of the node (Ω) for late deployment. Figure 16 and Figure 17 summarize 3B and 2B launch window performance penalties, respectively. The maximum performance/zero penalty (y = 0) reference point was an on-time launch (x = 0) and deployment on the 5th orbit (revolution) of the Space Shuttle. All other launch times (either early or late) and later deployment revolutions resulted in a performance penalty due to the out of orbital plane yaw steering which had to be done to correct the Ω. The ordinate axis was expressed in terms of change in pounds of propellant excess (PE), which was the additional Centaur propellant which had to be consumed to perform this nodal correction. Since the yaw steering constituted a loss in available performance, the ordinate was plotted as negative values. Performance losses were also calculated for two succeeding revolutions (6th and 7th). Each successive revolution had a performance loss due to $LH_2$ propellant boil-off (thus the vertical shift downward for each curve). The optimum of each revolution also shifted to a later time due to nodal regression. The park orbit inclinations used for the 3B and 2B cases were 37° and 57°, respectively.

The 3B and 2B launch window performance penalty curves varied considerably. Comparing the ordinates, a 45 min early launch with a revolution 7 deployment produced a ~170 lb PE penalty for the 3B transfer, yet the penalty for the same conditions was ~ 550 lb of PE for a 2B transfer. If a Launch Time Reserve (LTR) of only 100 lb was available, then the launch window using a 3B transfer could be as long as ~70 min for a deployment on revolutions 5 through 7. For a 2B transfer, however, the same LTR would only enable a ~28 min window. The 3B and 2B LTR's for three fixed window lengths are shown in Table 6. For the same range of revolutions (5, 6, and 7), the longer the window, the more desirable the 3B transfer became. Example: the LTR for a 15 min 2B window (~ 48 lb) would be more than enough for a 30 min 3B window (~ 37 lb), whereas a 1 hr 2B window (~ 320 lb) would be more than four times the LTR as a 1 hr 3B window (~ 78 lb). The advantage of a 3B transfer was not just significantly better performance due to lower LTR propellant needed to be held in reserve, but also improved launch operations by increasing tolerance to launch delays, reducing the chance of scrubbing a launch.

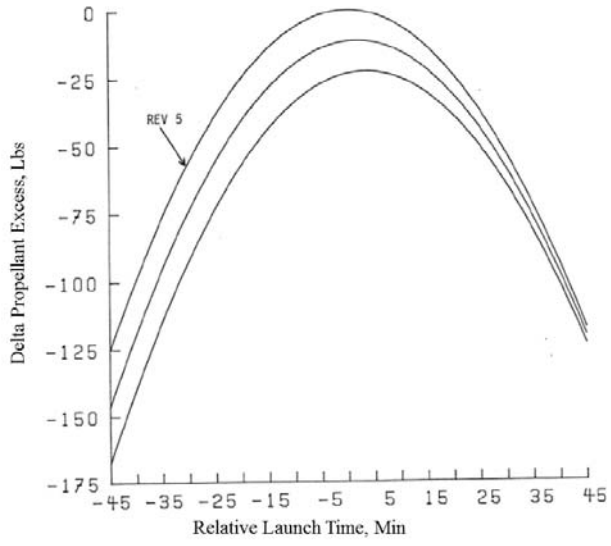


Figure 16.—Launch Window Performance Penalties for 3B Transfer.

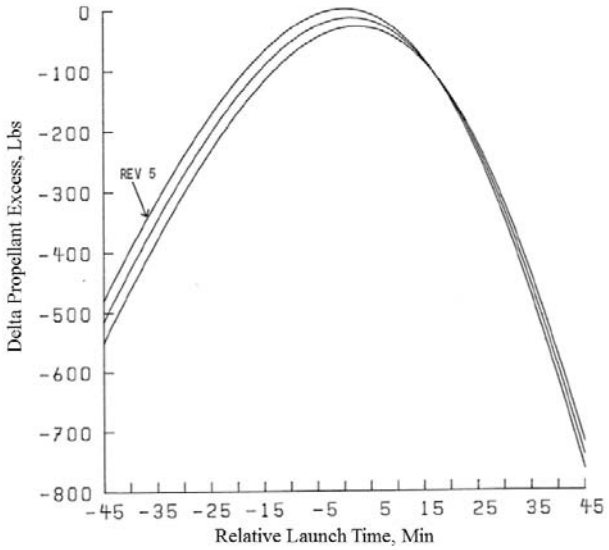


Figure 17.—Launch Window Performance Penalties for 2B Transfer.

TABLE 6.—LAUNCH WINDOW PENALTIES FOR 3B AND 2B TRANSFERS

| | Window Length (min) | PE Penalty (lb) | Window Opens (min) | Opening Rev | Window Closes (min) | Closing Rev |
|---|---|---|---|---|---|---|
| 3 Burn | | | | | | |
| | 15 | –26.3 | –4.0 | 7 | 11.0 | 7 |
| | 30 | –36.7 | –11.5 | 7 | 18.5 | 7 |
| | 60 | –77.7 | –26.2 | 7 | 33.8 | 7 |
| 2 Burn | | | | | | |
| | 15 | –47.7 | –5.3 | 7 | 9.7 | 7 |
| | 30 | –103.4 | –13.4 | 7 | 16.6 | 7 |
| | 60 | –320.4 | –31.1 | 7 | 28.9 | 5 |

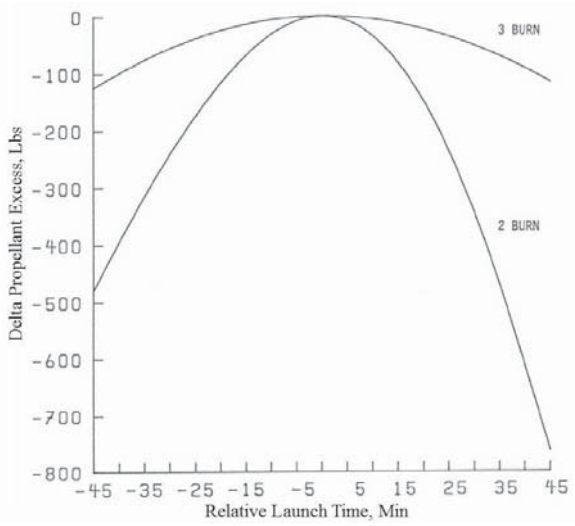


Figure 18.—Launch Window Performance Penalties for 3B Versus 2B Transfers (Rev 5 Only).

For the 2B transfer, most of the node correction was performed by Burn 2. This would be expected since out of plane thrusting is more efficient at low velocities (thus higher altitudes). The curve in Figure 20 is almost linear with a negative slope, where early launches would need increased (easterly rotated) nodes and vice versa. At $t$ = +27.4 min, however, the curve passed through zero due to the geographic location at the equator. (The Ω cannot be changed when the position is already at the node.) Around that location, the Ω shift had to be done solely by Burn 1. This was manifested by the minima in Figure 19 which corresponded to this point. Though barely visible, inflection points are present in Figure 20 which corresponds to both points of zero Ω change in Figure 19. These are not due to the geographic position Burn 1, but rather the change in sign in optimal Ω shift by Burn 1.

For the 3B transfer (similar to 2B), most of the Ω correction was done by the mostly out of plane Burns 2 and 3, with only a small amount (~ 2½°) done by the in plane Burn 1 (Figure 21). Similar to the earlier discussion, the amount of Ω change was shared by Burns 2 and 3 in a more optimal way than 2B. For early launch, the Ω was over-corrected (increased; easterly rotated) by Burn 2, then reduced modestly by Burn 3. For late launch, the Ω was under-corrected by Burn 2 with the node further corrected (decreased; westerly rotated) by Burn 3. Since neither Burn 2 nor 3 were located near the equator, Burn 1 did not fluctuate as it did in 2B. Also, since there were no zero Ω change points throughout the window for any burn, there were no inflection points.

$$\frac{\partial \Omega}{\partial t} = \left[ \frac{r}{\sqrt{l\mu}} \frac{\sin(\theta + \omega)}{\sin i} \right] W \tag{5}$$

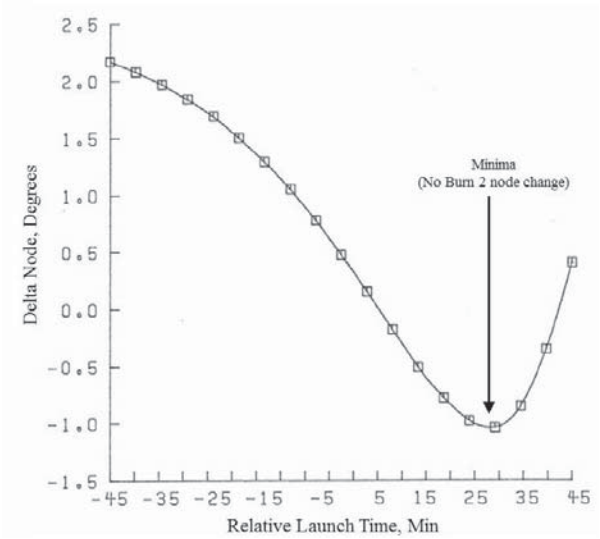


Figure 19.—Node Change in Launch Window During Burn 1 for 2B Transfer.

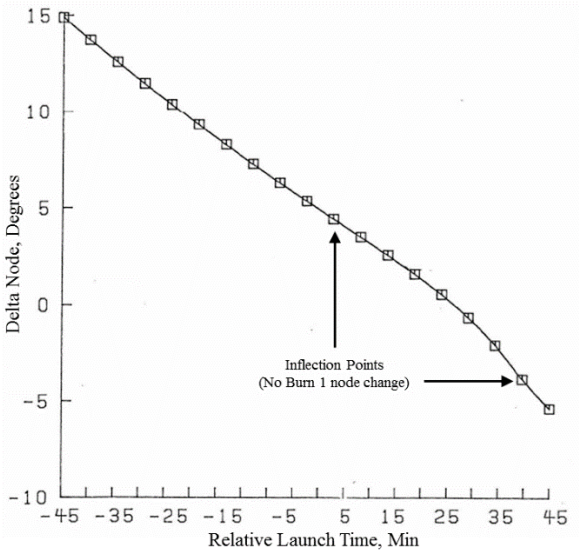


Figure 20.—Node Change in Launch Window During Burn 2 for 2B Transfer

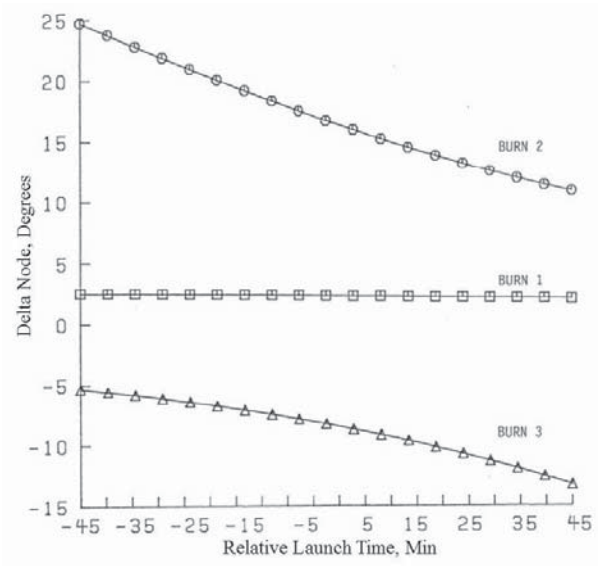


Figure 21.—Node Change in Launch Window During All Burns for 3B Transfer

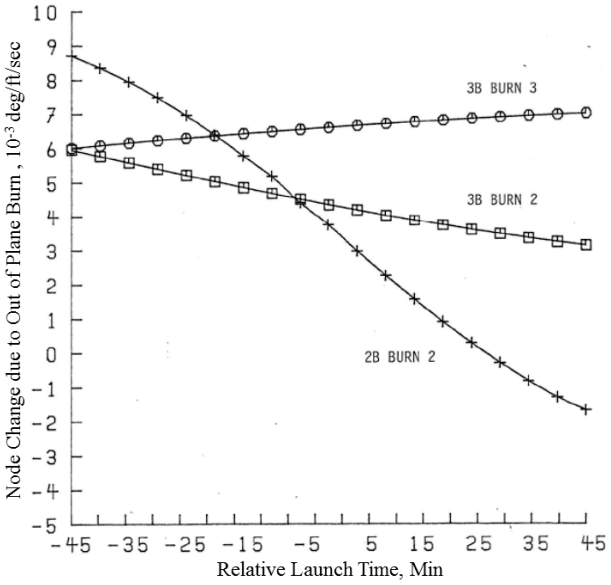


Figure 22.—Coefficients of Time Derivative of Node for Burns 2 and 3 for 3B Transfer and Burn 2 for 2B Transfer.

To better understand why the trajectory optimization arrived at these solutions, the same approach used in the earlier discussion on orbital element changes is used here (employing a time derivative of an orbital element as a function of thrust components). Equation (5) is the time derivative for Ω and is seen to be solely a function of out of orbital plane (yaw) thrusting (Ref. 11). It was plotted in Figure 22 (analogous to the data in Table 3) using data from the launch window trajectories of Burns 2 and 3 for the 3B and 2B transfers. Over most of the opportunity, 2B was not as efficient in changing Ω compared to 3B, as the 3B Burn 3 values exceeded $6\times10^{-3}$ deg/ft/sec. For early launches, there was less of a difference between 3B's Burns 2 and 3. However, for very early launches ($-45 < t$ (min) $< -25$), 2B had more favorable conditions with values exceeding $9\times10^{-3}$ deg/ft/sec. Nevertheless, the benefit of splitting up the

yaw over Burns 2 and 3 in 3B more than compensated for the slightly unfavorable orbital elements present in the early part of the window. In order to understand how each of the orbital elements effected Equation (5) throughout the windows, Figure 23 to Figure 26 show θ, ω, sin(*u*), and '*r*' as functions of launch time for Burns 2 and 3 for the 3B and 2B transfers (argument of the latitude $u = \theta + \omega$). The inclination and semi latus rectum were fairly constant throughout the window. Note in Figure 23, 3B's Burn 3 was plotted negatively to enable viewing on the same axis.

For the 2B transfer, the orbital elements for early launch were such that the nodal time derivative values were greater for 2B than those of the 3B transfers. Burn 2 for both 2B and 3B was greatly out of plane and positive, which enabled the Ω to be moved move readily in an eastwardly direction to correct for early launch. Sin(*u*) and '*r*' were greater for 2B than 3B, which enabled easier Ω correction (i.e., greater Eq. (5) values).

For late launch, however, the situation was quite different. Since Ω had to be reduced (rotated westerly) relative to the node at $t = 0$ for positive out-of-plane thrust angle, θ had to be reduced greatly in order for the argument of the latitude to go negative (thus sin(*u*) to go negative). This is apparent in Figure 23 where θ dramatically decreased, from 128° for on-time launch ($t = 0$) to 66° for a 45 min late launch. Since ω was negative and close to the final Molniya value (Figure 24), this large change in θ drove the '*u*' from 36° to –40°, which drove sin(*u*) from 0.59 to –0.63 (Figure 25). The θ change also greatly decreased '*r*', because of the highly eccentric orbit ($e = 0.715$). For every 5 min delay in launch, the radius at which Burn 2 took place decreased by approximately 470 nmi at window opening and 445 nmi at window closing, and by ~950 nmi at mid-window. In total, the altitude decreased from a high of 14,740 nmi at window open to 1,270 nmi at window close (Figure 26). As launch time became later, Burn 2 shifted toward node, crossing the equator, and then preceded the node (i.e., moved into the southern hemisphere). The combined effect of these changes was a large reduction in the time derivative of the Ω for late launch, driving up the performance penalty for 2B transfer. While the combined changes in '*r*' and sin(*u*) drove Equation (5), it was primarily the decrease in '*r*' which drove the time derivative of Ω as can be seen by comparing the curves in Figure 22 to Figure 26. This also explains the severe asymmetry of the 2B curve in Figure 18, where late launch was significantly more costly than early launch (–765 vs. –480 lb of PE, respectively).

For the 3B transfer (unlike 2B) the Ω change was shared by Burns 2 and 3 as was seen in the baseline case. Figure 23 shows that θ remained almost constant throughout the launch window. (Note that Burn 3 was plotted with negative values to facilitate plotting both curves on the same axis.) θ varied only 9° from early to late launch for Burn 2, and only 4° for Burn 3. ω was similarly invariant, shifting less than 8° for Burn 2 and 1° for Burn 3 (Figure 24). Thus sin(*u*) was relatively invariant and of opposite slope for Burns 2 and 3, permitting flexibility in nodal correction (Figure 25). The radius for 3B transfer gradually decreased for Burn 2 and gradually increased for Burn 3, but both were relatively high and relatively invariant when compared to the large altitude changes in Burn 2 in 2B (Figure 26). Indeed, Burn 2 varied only 2,770 nmi over the entire 1½ hr opportunity. Burn 3 always took place at a greater altitude than Burn 2 and vacillated even less. This permitted the change in Ω to be optimally distributed over Burns 2 and 3. Since the out-of-plane component of Burn 3 was negative (opposite of the angular momentum vector), the Ω could readily be moved westerly for late launches. So for the 3B transfer, a considerable amount of node change could be done over a widespread stretch of launch time and not result in a greatly diminished time derivative of node change as in 2B.

In summary, whether the goal is a longer window, smaller LTR, more deployment revolutions, or a combination of all three, 3B was significantly superior to 2B. For heavy payloads, where the LTR might be limited, this could mean the difference between a generous launch/deployment period with adaptability to ground operation delays, and a constricted launch opportunity inflexible to obstacles impeding launch.

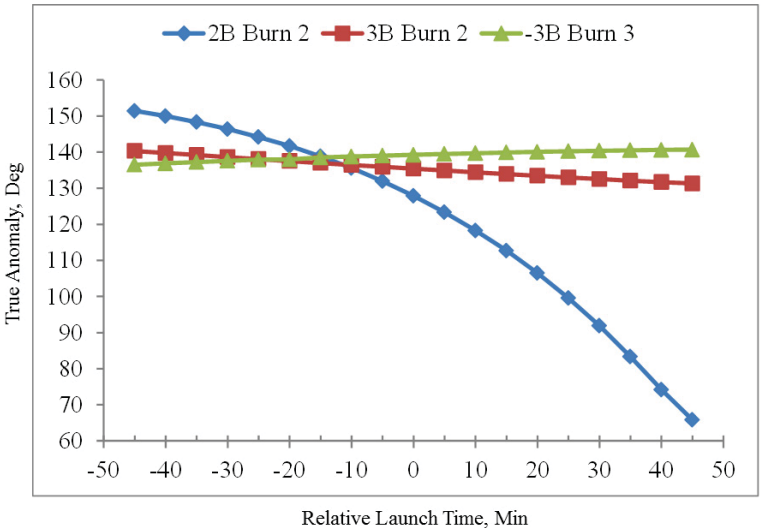


Figure 23.—True Anomaly Change in Launch Window During Burns 2 and 3 for 3B Transfer and Burn 2 for 2B Transfer.

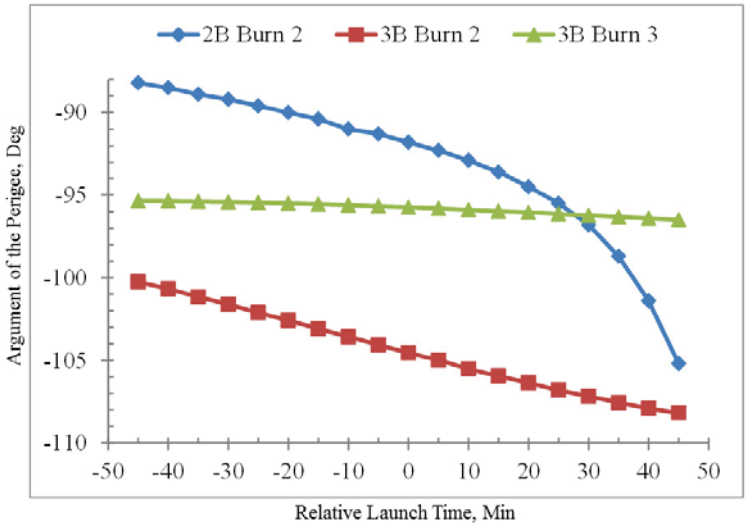


Figure 24.—Argument of the Perigee Change in Launch Window During Burns 2and3 for 3B Transfer and Burn 2 for 2B Transfer.

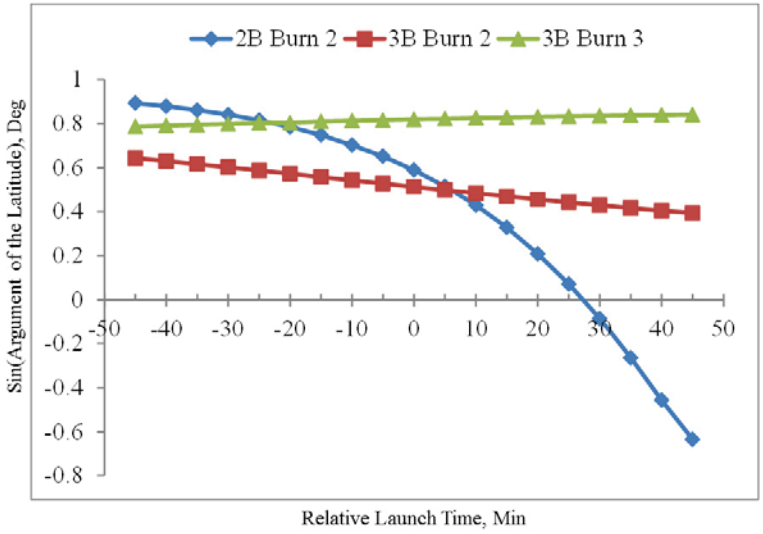


Figure 25.—Sin(Argument of the Latitude) Change in Launch Window During Burns 2and3 for 3B Transfer and Burn 2 for 2B Transfer.

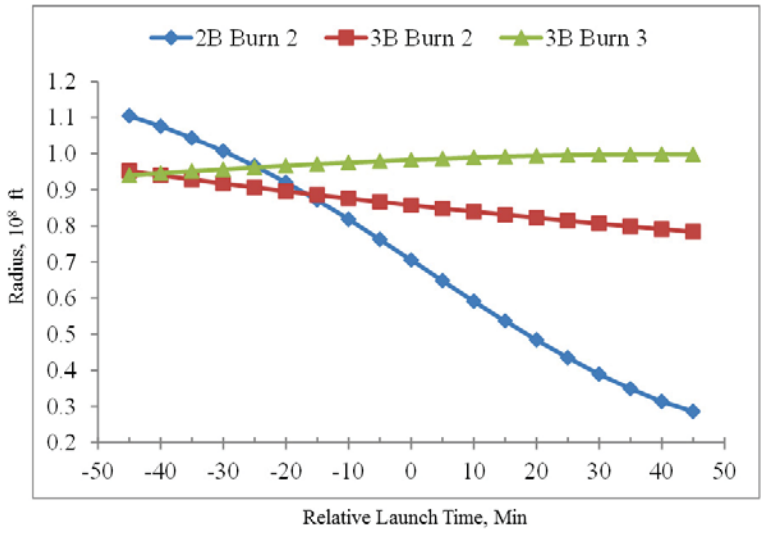


Figure 26.—Radius Change in Launch Window During Burns 2and3 for 3B Transfer and Burn 2 for 2B Transfer.

## 6.0 Ground Tracks

Ground tracks were calculated for 2B and 3B transfers using the orbit/trajectory visualization software KPLOT from the NASA Jet Propulsion Laboratory based on results from DUKSUP.14 This analysis included burn and coast phases as well as their variation within a 90 min launch window. The ground track of the nominal (i.e., on-time) 2B transfer is shown in Figure 27. The longitudinal position was largely a function of the parking orbit state vector and deployment revolution. Thus for the standard park orbit ($i$ = 57°) and deployment revolution 5, Burn 1 took place halfway between South Africa and Antarctica. The long Burn 1 arc in LEO was located out of range of any ground tracking station and would necessitate one of two coverage options: the use of two Advanced Range Instrumentation Aircraft (ARIA) or the Tracking and Data Relay Satellite System (TDRSS) to secure telemetric data of the burns (or at least MES and MECO). The 2B ground track then passed through the southern Indian Ocean, skirting the western coast of Australia, through the Indonesian archipelago, passing southeast of the Philippines, culminating south of Japan where the Burn 2 ground track appeared as a short segment. Burn 2 should have been visible from the Guam Tracking Station (GTS (GWM)).

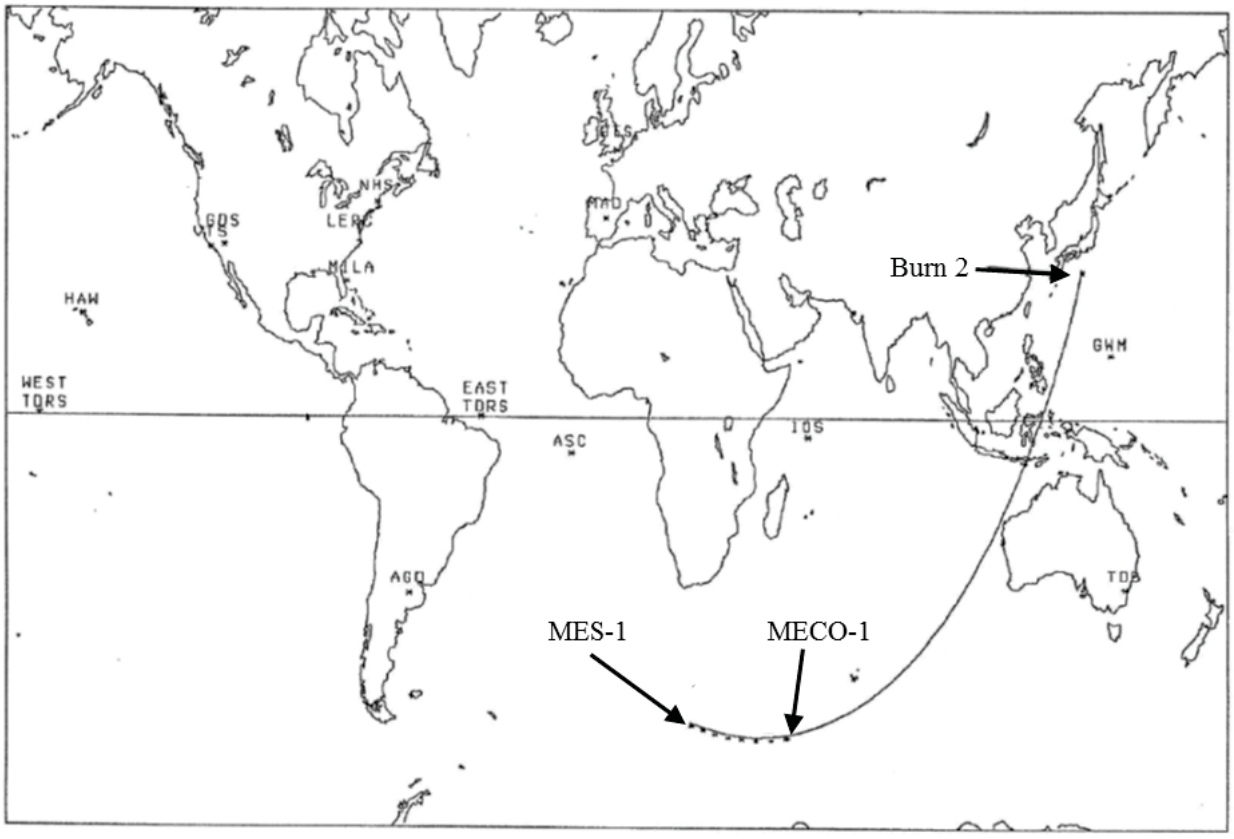


Figure 27.—Ground Track of 2B Transfer.

The ground track of the nominal 3B transfer is shown in Figure 28. For the park orbit ($i$ = 37°) and deployment revolution 5, Burn 1 took place between the eastern South American coast and South Africa. As with the 2B transfer, the long Burn 1 arc in LEO was located out of range of any ground tracking station and would also have necessitated either two ARIA aircraft or TDRSS. Following Burn 1, the 3B ground track then skirted the South African coastline and diagonally bisected (southwest to northeast) the Indian Ocean. Burn 2 appeared as a short segment over Burma, but because of its high altitude, it should have been visible to both Diego Garcia Station (DGS) (i.e., Indian Ocean Station (IOS)) and GTS. The ground track then moved north and slightly westward (due to its decreasing Earth-relative speed as it approached apogee), crossing over China and Russia. Following apogee, the track proceeded in a due south direction until Burn 3 took place between the Areal Sea and Lake Balkash in Kazakhstan. Again, due to its high altitude, Burn 3 should have been visible to ground stations in this hemisphere, including Telemetry and Command Station (TCS) (i.e., RAF Oakhanger (England) Tracking Station (OTS)).

There was one primary difference between 3B and 2B ascent profiles relative to the Earth. Unlike the 2B transfer, 3B's Burn 1 passed through the center of the South Atlantic Anomaly (Figure 29), a region of the Van Allen Radiation Belt in space which has an altitude as low as 108 nmi (Ref. 15). Proton (>50 MeV) fluxes in excess of 1000/(cm$^2$ sec MeV) could be experienced during Burn 1 (Ref. 15). Because of this, assessments on the tolerances of both the Centaur stage and spacecraft avionics to this higher radiation environment would be necessary.

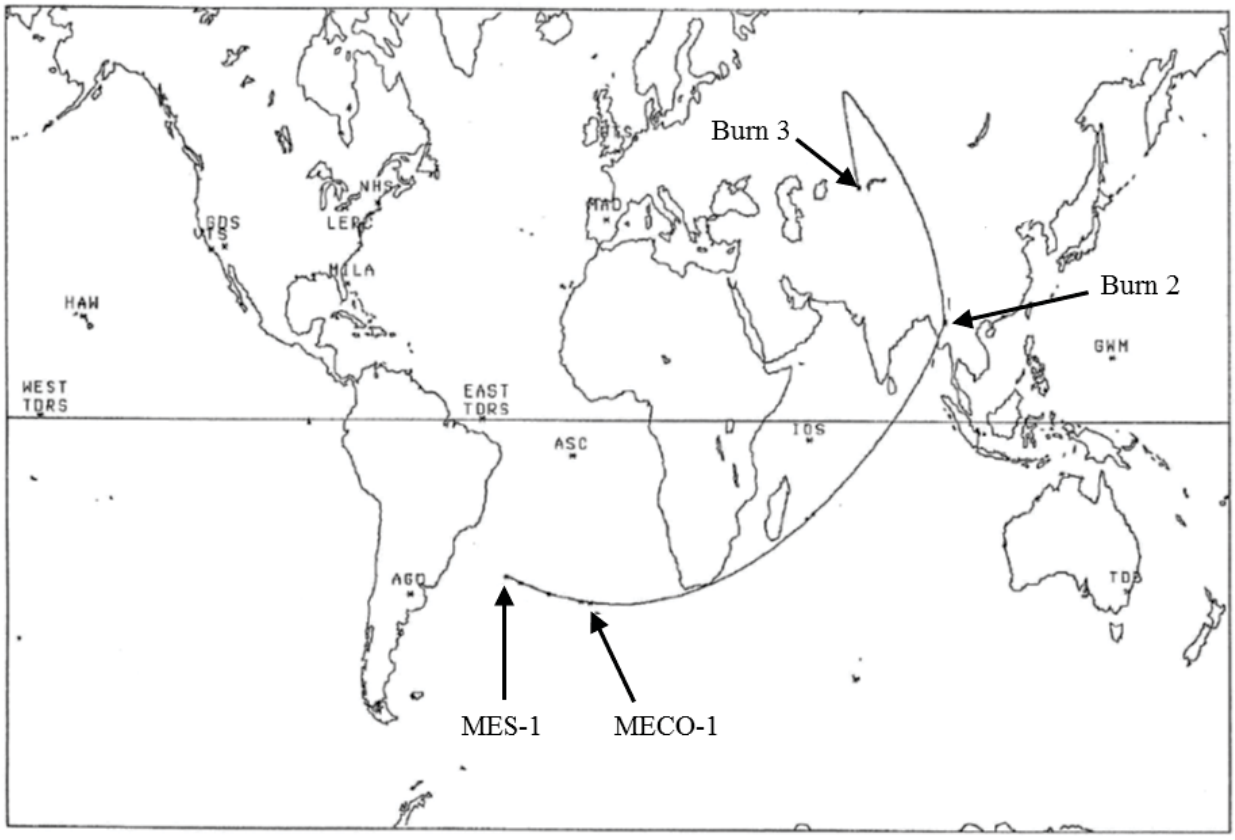


Figure 28.—Ground Track of 3B Transfer.

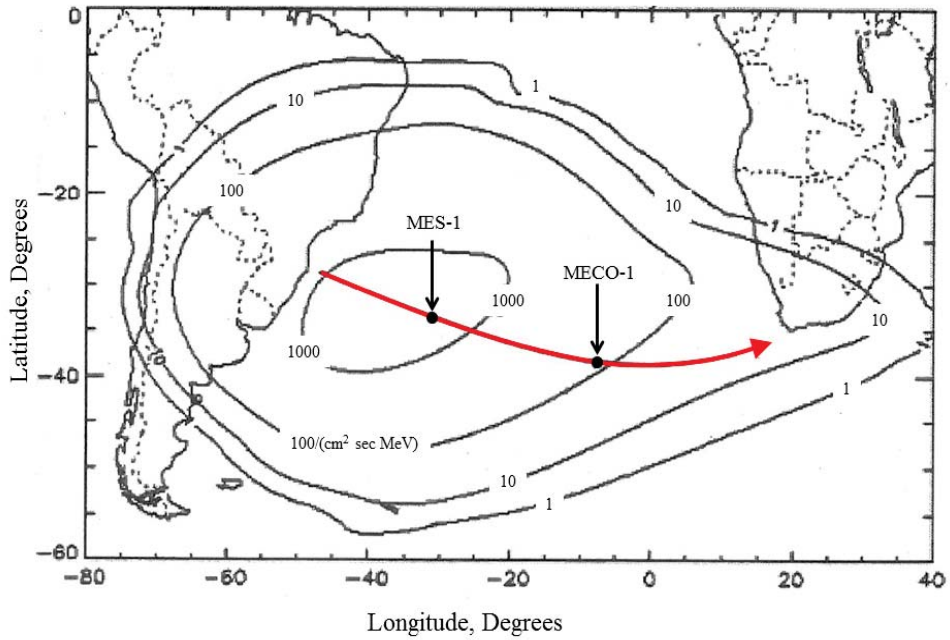


Figure 29.—3B Transfer Burn 1 Transit Through South Atlantic Anomaly.

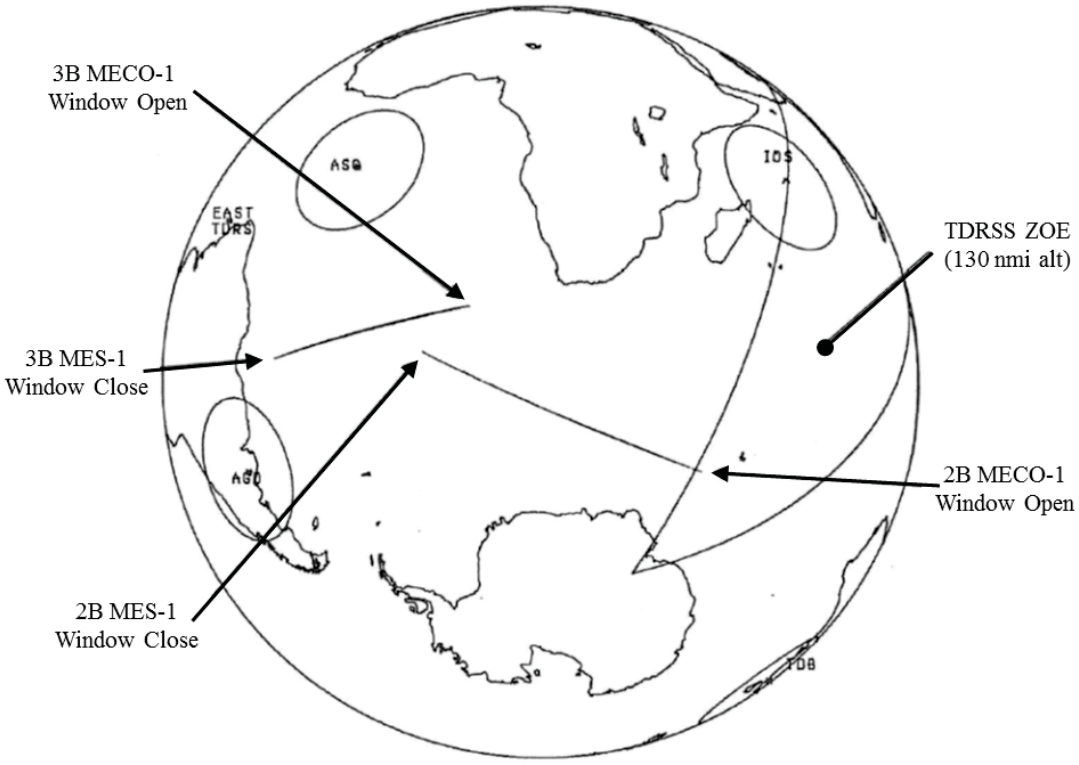


Figure 30.—Burn 1 Ground Tracks for 3B and 2B Transfers Through Launch Window.

The range of ground tracks for Burn 1 for both 2B and 3B as they varied throughout a 90 min launch window are shown in Figure 30. In both 2B and 3B transfers, the western-most start of the Burn 1 ground track was MES at window close (i.e., 45 min late launch), while the eastern-most end of the Burn 1 ground track was MECO at window open (i.e., 45 min early launch). The burns throughout the windows

were coincident on the same arc, differing only in start and stop points. The nominal (on time) burn arcs were located in the center of the arcs shown in Figure 30. All ground tracks shared the same tracking limitations as the mid-window (on time) ascents. Note however that MECO-1 for 2B at the opening of the launch window intruded slightly into the TDRSS Zone of Exclusion for that altitude. Because of the wide range of ground tracks through the window, additional ARIA might have been necessary for adequate coverage of the first burn.

The range of ground tracks for Burns 2 and 3 for both 2B and 3B throughout a 90 min launch window are shown in Figure 31. Due to the shortness of the burns, most of the ground tracks appeared as short segments or dots (i.e., MES and MECO were almost indistinguishable). Their range from launch window open to close, however, was considerable compared to their burn arcs. 2B's Burn 2 varied the most, from the west coast of Australia at window close to the Sea of Okhotsk north of Japan at window open. Recalling the earlier discussion on the variation of '*r*' and θ within the window (which drove the wide change in latitude), TDRSS support would be mandatory for 2B's Burn 2 since ARIA would not have been able to accommodate such a span of ground tracks. Also, given the relatively low altitude at window close, GTS would not likely be visible. 3B's Burns 2 and 3 were not as dispersed as Burn 2 of 2B's for the same reason as discussed earlier regarding out of plane yaw. 3B's Burn 2 ranged from the Bay of Bengal at window close to central China at window open. 3B's Burn 3 ranged from east of the Areal Sea at window close to south of Lake Balkash at window open, all within Kazakhstan. As with Burn 1, the nominal (on time) burn arcs were located in the center of the arcs shown in Figure 31, though Burn 2 of 2B was more geographically offset (as shown). All burns (except 2B's Burn 2 late launch) were expected to be similarly visible to ground stations as the mid-window (on time) ascents because of their high altitude.

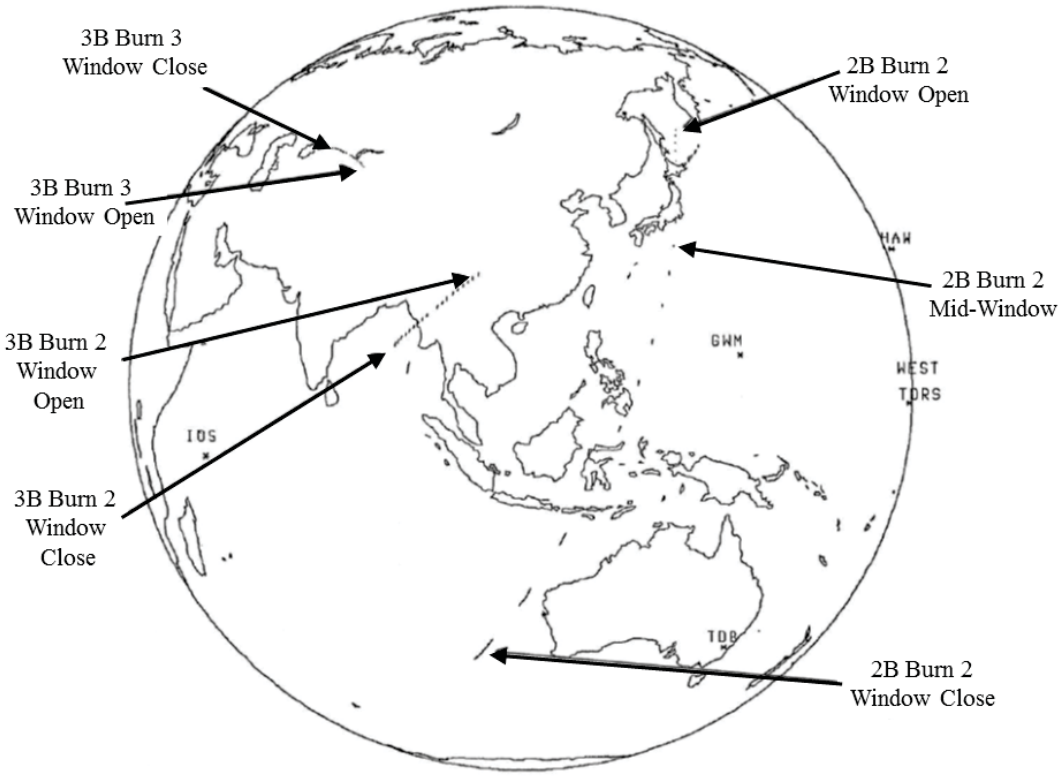


Figure 31.—Burns 2 and 3 Ground Tracks for 3B and 2B Transfers Through Launch Window.

In summary, both 2B and 3B would require similar tracking assets (ARIA or TDRSS) for Burn 1. For the 2B transfer, Burn 2 would need TDRSS for a 90 min launch window. Only with a significantly shortened window would Burn 2 be visible from a station such as GTS. For the 3B transfer, Burns 2 and 3 should be visible from various ground stations throughout a 90 min launch window. This is despite the considerable differences in geographic over-flight locations. The 3B transfer, however, did have an additional operational concern pertaining to flight through the center of the South Atlantic Anomaly during Burn 1.

## 7.0 Relevance to Future Missions

While the Shuttle/Centaur G vehicle never flew, this analysis has a few potential applications to future missions. As was mentioned, all ELVs' lift capabilities are degraded as launch azimuth is decreased from 90° due East. Should another booster and upper stage combination find itself in a similar situation in attempting to perform a performance-demanding Molniya (or similar) mission, most of the orbital mechanics and engineering analysis contained in this study should still be relevant. Another application pertains to national security interests, which might find interesting the impacts of on-orbit loitering analogous to the Space Shuttle's multiple revolution operations prior to upper stage/payload deployment. Further, a transfer such as 3B to Molniya could help "camouflage" the transfer orbit. Lastly, it is believed by the author that this paper represents one of the few documents explaining the physics of finite launch windows combined with multiple revolution space operations for a generic Molniya mission in the open literature. Thus, this material should be useful for certain future applications.

## 8.0 Conclusions

While it has been almost 30 years since the joint NASA-USAF Shuttle/Centaur program developed stages for performance-demanding missions such as Molniya orbit, much of the analytical work was never documented. The unconventional three orbital burn transfer to Molniya orbit was one of those works. This alternate transfer was pursued primarily to mitigate a major concern of the time pertaining to propellant slosh-dynamics during deployment from the Shuttle cargo bay. Today, however, the performance and orbital mechanics of this transfer should be of interest academically, and also may have applications for future national security missions.

The most unusual characteristic of the three burn (3B) transfer was that the total energy of its second transfer orbit was significantly greater than that of the final orbit. This was unusual among orbit transfers, which typically are monotonically increasing in orbital energy. But it was nevertheless optimal because of how the optimization performed the out of plane maneuvers to satisfy angular orbital element ($i$ and $\omega$) requirements in a more efficient way than could be done in the two burn (2B) transfer. Thus the 3B transfer with comparable performance to the 2B transfer existed because it was advantageous to increase '$a$' and $R_p$ beyond their target values, only to subtract them back out in order to split up and perform the inclination and $\omega$ changes in more favorable orbital element spaces.

The Centaur with fully loaded propellant tanks could be flown from a 37° inclination low Earth parking orbit via a 3B transfer to achieve Molniya orbit with comparable performance to the base-lined 2B transfer (9,545 vs. 9,552 lb of separated spacecraft weight, respectively) which started from a 57° inclined orbit and required a 40 percent propellant offload. There was a significant reduction in the need for propellant launch time reserve for a 1 hr window: only 78 lb for the 3B transfer versus 320 lb for the 2B transfer. This also meant that longer launch windows over more orbital revolutions could be done for the same amount of propellant reserve. These performance results were due to 3B's ability to more optimally distribute the out-of-orbital plane steering changes in inclination, $\omega$, and $\Omega$ over three burns

rather than just two. While the 3B versus 2B ground tracks varied considerably, there was no practical difference in ground tracking station or airborne assets needed to secure telemetric data, even though the geometric locations of the burns varied considerably. One potential issue was that the first burn of the 3B transfer would traverse the most intense region of the South Atlantic Anomaly, requiring an assessment of the impacts of this high radiation environment on both Centaur and payload. The 3B transfer did entail a significant adverse increase in total mission time compared to 2B (12 vs. 1¼ hr). However, the longer transfer time could be accommodated by using existing (though optional) payload batteries (necessitating a significant performance hit), using unallocated reserves in hydrazine RCS propellant, and swapping helium pressurent bottles.

Finally, it is important to acknowledge the satisfying of the primary objective of the study: to establish the validity of the hypothesis that the 3B transfer could perform the Molniya mission with comparable performance while fully loading the propellant tanks on Centaur. As is illustrated in the summary Table 7, a reasonable case could be made that (all issues considered) the 3B transfer would have been preferable to the baselined 2B transfer.

TABLE 7.—SUMMARY FIGURES OF MERIT FOR 3B VERSUS 2B TRANSFERS

| | 3 Burn | 2 Burn |
|---|---|---|
| Propellant Loading | Full tanks | 40% offload |
| Payload (lb) | 9,545 | 9,552 |
| Mission elapse time (hr) | 12 | 1 1/4 |
| Launch window (1 hr) (lb PE) | 78 | 320 |
| Ground tracks (nominal) | SAA intrusion | Manageable |
| Ground tracks (nominal) | Manageable | Burn 2 span |
| Vehicle modifications | Battery harness; He bottle swap; ~210 lb total hit | None |

# Appendix A.—Three Burn and Two Burn Propellant Tanking Information (All Modeling Taken From Mini-Colt (Ref. 3)

***For 3 Burn:***

WPMAX = maximum allowable main impulse propellant
= total tankable – settlings – residuals – CVR for 12 hr mission – FPR (from full tanked mission)
= 30,366 – 806 – 413 – 188 – 260
= 28,699 lb

Inclination where initial weight = weight limit defined point where offloading of $LO_2$ began (at $i$ = ~35.75°)
Inclination where offloading of both $LO_2$ and $LH_2$ defined by:

$$\frac{(LO_2)_{max-x}}{(LH_2)_{max}} = 6.0 = \frac{25{,}075 - x}{4{,}072} \text{ yields } x = 643 \text{ lb}.$$

Thus 28,699 – 643 = 28,056 lb at $i$ = ~36.75°

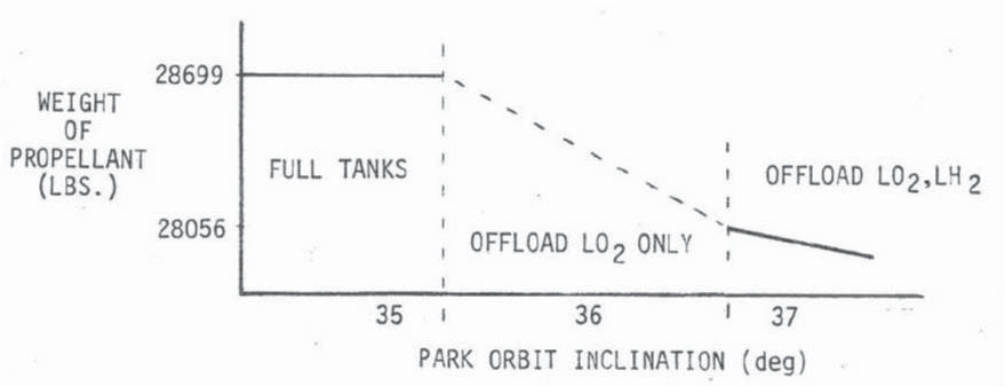


***For 2 Burn:***

WPMAX = 30,366 – 573 – 413 – 188 – 260 = 28,932 lb

$$\frac{25{,}222 - x}{4{,}158} = 6.0 \text{ yields } x = 274 \text{ lb}$$

At 28932 – 274 = 28,658 lb. began offloading both $LO_2$, $LH_2$. This occurred at 37° > $i$ > 38°.

FPR = Flight Performance Reserve
CVR = Centaur Vehicle Reserve

# Appendix B.—RL10 Propulsion System Modeling

In fully tanked region of inclinations, the RL10A-3-3B engine characteristics are:

***For 3 Burn:***

$$O/F = \frac{25{,}075}{4{,}072} = 6.1579$$

Thrust = 30,130.74 lb
WTFLOW = 68.6937 lb/sec

***For 2 Burn:***

$$O/F = \frac{25{,}222}{4{,}158} = 6.0659$$

Thrust = 30,130.74 lb
WTFLOW = 68.6937 lb/sec

In offloaded region of inclinations:

***3 Burn and 2 Burn:***

O/F = 6.0
Thrust = 30,036.0 lb
WTFLOW = 68.25 lb/sec

# Appendix C.—Net Payload Calculations
# (All Constants Were Taken From mini-Colt (Ref. 3)

"wet Centaur" = dry Centaur + FPR + CVR + residuals

***For full tanks, both 3 Burn and 2 Burn:***

Payload = burnout weight – wet Centaur
= burnout weight – (dry Centaur + FPR + CVR + residuals)
= WF – ( 6,574 + 260 + 188 + 53 )
= WF – 7,533

***For offloaded region, both 3 Burn and 2 Burn:***

Payload = WF – ( 6,574 + 260 + 454 + 550 )
= WF – 7,838

WF = "burnout weight"
FPR = Flight Performance Reserve
CVR = Centaur Vehicle Reserve

# Appendix D.—$LH_2$ Boiloff Modeling and Reaction Control System (RCS)

***For 3 Burn:***

$LH_2$ boiloff rate was extrapolated from geosynchronous (GEO) mission

Using 19 lb/5.08 hr:

1st transfer orbit coast phase vent = 8.2 lb.

2nd transfer orbit coast phase vent = 44.5 lb

For fully tanked mission

| | |
|---|---|
| $N_2H_4$ pre MES-1 | = pre MES-1 for fully tanked mission (GEO) |
| $N_2H_4$ pre MES-2 and pre MES-3 | = pre MES-2 for GEO |
| $N_2H_4$ post MECO-2 and post MECO-3 | = post MECO-2 for offloaded mission (Molniya) |

For offloaded region:

| | |
|---|---|
| $N_2H_4$ pre MES-1 | = pre MES-1 for fully tanked mission (GEO) |
| $N_2H_4$ pre MES-2 | = pre MES-2 for GEO |
| $N_2H_4$ pre MES-3 | = pre MES-3 for Molniya |

***For 2 Burn:***

All fuel ventings and RCS propellants were kept at the same values given in mini-Colt 6 for Molniya mission.

Offloaded and fully tanked regions were modeled the same.

# Appendix E.—Approximation by Drop Masses

Masses which are dropped at the end of Transfer Orbits 1 and 2 ($M_{D1}$ and $M_{D2}$, respectively) could be used to approximate the pre-chill, pre-start, and start-up transients which, while significant consumers of propellant, contributed little $\Delta V$ for the mission. Using fixed $\Delta V$s for all three burns (taken from integrated computer runs for park orbit at $i$ = 37°), the mass ratios ($L_2$ and $L_3$) for Burns 2 and 3, respectively, were given by:

$$L_2 = \frac{M_{prop2} + (M_{PL} + M_{ST})(L_3 - 1) + M_{D2} + M_{PL} + M_{ST}}{(M_{PL} + M_{ST})(L_3 - 1) + M_{D2} + M_{PL} + M_{ST}}$$

$$L_3 = \frac{M_{prop3} + M_{PL} + M_{ST}}{M_{PL} + M_{ST}}$$

Substituting these expressions into the rocket equation representing the total $\Delta V_T$ of all three burns resulted in the expression (where $M_T$ is total initial mass which is a constant, $\Delta V_T$ = 13,502.5 ft/sec = constant, and RL10 $I_{sp}$ = 440.1 sec from Appendix B):

$$L_2 L_3 (M_{PL} + M_{ST}) + L_2 M_{D2} + M_{D1} = L_2 L_3 M_T e^{-\Delta V_T / g_c I_{sp}}$$

Differentiating with respect to each drop mass separately yielded (for fixed $\Delta V$'s from integrated runs):

$$\frac{\partial M_{PL}}{\partial M_{D1}} = \frac{-1}{L_2 L_3} = -0.67$$

$$\frac{\partial M_{PL}}{\partial M_{D2}} = \frac{-1}{L_3} = -0.9$$

Where:

$M_{PL}$ is payload mass
$M_{D1}$ and $M_{D2}$ are drop masses (losses) at the end of transfer orbits 1 and 2, respectively
$L_2$ and $L_3$ are mass ratios for Burns 2 and 3, respectively
$M_{prop}$ is the propellant mass for each burn

For vanishing 3B transfer at park orbit with $i$ = 57°, these partials were in the limit −0.9 and −1.0, respectively.

## References


1. Stofan, A. J., “A High Energy Stage for the National Space Transportation System,” NASA TM 83795, 1984.
2. “Shuttle/Centaur Program,” General Dynamics Convair Division, San Diego, CA, 1983.
3. Williams, C. H., “Generic Shuttle/Centaur G Vehicle/CISS Configuration, Weight, and Performance Baseline and Status” (“mini-Colt”), USAF Space Division Detachment OLAC at NASA Lewis Research Center, issue No. 6, Cleveland, OH, Sept. 1984.
4. “Centaur Vehicle Simulation Data Book,” General Dynamics Convair, Report No. GDC-SP-84-002, San Diego, CA, Mar 1984.
5. “Shuttle/Centaur G Level III/IV Critical Design Review at LeRC,” General Dynamics Space Systems Division, San Diego, CA, Oct 1984.
6. “Centaur Vehicle Simulation Data Book (G Configuration),” General Dynamics Space Systems Division, Report No. GDSS-SSC-85-005, Contract NAS3-22901, San Diego, CA, May 1985.
7. “Shuttle/Centaur G Configuration, Performance, and Weight Status Report” (“Colt”), General Dynamics Space Systems Division, Report No. GDSS-SSC-85-006-2, Contract NAS3-3322, San Diego, CA, Oct 1985.
8. Zondervan, K. P., “Optimal Low Thrust, Three Burn Orbit Transfers with Large Plane Changes,” Ph.D Thesis, California Institute of Technology, Pasadena, CA, 1983.
9. Spurlock, O.F., Teren F., “Optimum Launch Trajectories for the ATS-E Mission,” NASA TM X-52836, NASA Lewis Research Center, July 1970.
10. Spurlock, O. F., Williams, C.H., “DUKSUP: A Computer Program for High Thrust Launch Vehicle Trajectory Design & Optimization,” AIAA Propulsion and Energy Forum and Exposition 2014: 50th AIAA/ASME/SAE/ASEE Joint Propulsion Conference, American Institute of Aeronautics and Astronautics, pre-print, Control ID#: 1943459, Cleveland, OH , July 2014.
11. Dobson, W.F., Huff, V.N., Zimmerman, A. V., “Elements and Parameters of the Osculating Orbit and Their Derivatives,” NASA Technical Note D-1106, NASA Lewis Research Center, Jan 1962.
12. Labuszewski, T.E., “ETR STS Payload Capability vs. Inclination for “Centaur Type” Missions,” Internal letter, Rockwell International, Satellite Systems Division, Downey, CA, 30 Oct 1984.
13. Hill, T. J., “Proposed Change to G-Generic Centaur Power Requirements,” NASA LeRC Engineering Review Board Request data package, ERB No. 6342-70, Nov 1985.
14. Schlaifer, R. S., Skinner, D. L., “KPLOT Users’ Manual,” NASA Jet Propulsion Lab, Release 1, with JPL correspondence (Diehl, R.) Jan 1984.
15. South Atlantic Anomaly intensity map, http://www.estec.esa.nl/wmwww/wma/rad_env.html